University of Nevada, Reno

Unscented Transformation-based Probabilistic Optimal Power Flow

A thesis submitted in partial fulfillment
of the requirements for the degree of

MASTER OF SCIENCE IN ELECRICAL ENGINEERING

By

Chenxi Qiao

Dr. Hanif Livani/Thesis Advisor

December, 2015

THE GRADUATE SCHOOL

We recommend that the thesis
prepared under our supervision by

CHENXI QIAO

Entitled

Unscented Transformation-based Probabilistic Optimal Power Flow

be accepted in partial fulfillment of the
requirements for the degree of

MASTER OF SCIENCE

Hanif Livani, Advisor

M. Sami. Fadali, Committee Member

Thomas Quint, Graduate School Representative

David W. Zeh, Ph.D., Dean, Graduate School

December, 2015

ABSTRACT

Renewable energy-based generation causes uncertainties in power system operation and planning due to its stochastic nature. The load uncertainties combined with the increasing penetration of renewable energy-based generation lead to more complicated power system operations. In power system operation, optimal power flow (OPF) is a widely-used tool in Energy Management System (EMS), for scheduling power generation of power plants, to operate the power system with least cost of generation and to ensure the security and reliability of power transmission grids. On the other hand, in order to deal with the stochastic variables (e.g., renewable energy-based generation and load uncertainties), probabilistic optimal power flow (POPF) has been instituted.

This thesis introduces a new Unscented Transformation (UT)-based POPF algorithm. UT-based OPF has a key advantage in handling the correlated random variables, and has become an open research area. Integrated wind power and independent or correlated loads are represented using a Gaussian probability distribution function (PDF). The UT is utilized to generate the sigma points that represent the PDF with a limited number of points. The generated sigma points are then used in the deterministic OPF algorithm. The statistical characteristics (i.e. means and variances) of the UT-based POPF solutions are calculated according to the inputs and their corresponding weights. Different UT methods with their corresponding sigma point selection processes are evaluated and compared with Monte Carlo Simulation (MCS) as the solution benchmark. In the thesis, Locational Marginal Price (LMP) in the transmission network is evaluated as the output of the UT-based POPF. The proposed algorithm is successfully verified on the standard IEEE 30- and 118-bus power transmission systems with wind power generation and unspecified loads. These two test cases represent a portion of American Electric Power (AEP) transmission grid.

ACKNOWLEDGEMENT

I would express my sincere appreciation to my advisor, Dr. Hanif Livani, for his support and patience. This thesis would not be possible without his guidance and help.

I would like to thank my committee members, Dr. M. Sami Fadali and Dr. Thomas Quint for their help in and out of the classes.

I want to thank Dr. Mehdi Etezadi-Amoli, and other faculty members in the Electrical and Biomedical Engineering department at University of Nevada, Reno.

Finally, I would also grateful to my family members, my parents, and my sisters, for their encouragement and endless support.

TABLE OF CONTENTS

TABLE OF FIGURES

LIST OF TABLES

LIST OF SYMBOLS

AEP	American Electric Power
DOE	Department of Energy
EMS	Energy Management System
ISO	Independent System Operator
LMP	Location Marginal Price
LSE	Load Serving Entities
MCS	Monte Carlo Simulation
MISO	Midcontinent Independent System Operator
OPF	Optimal Power Flow
PE	Point Estimation
PF	Power Flow
POPF	Probabilistic Optimal Power Flow
PDF	Probability Distribution Functions
RTO	Regional Transmission Organization
RPS	Renewable Portfolio Standard
STD	Standard Deviation
TO	Transmission Owners
UT	Unscented Transformation

CHAPTER 1

INTRODUCTION

1.1.Motivation

Power flow (PF) is an important tool to calculate power system operating conditions (i.e. voltage magnitude and angle). Optimal power flow (OPF) was introduced to minimize the cost of power system operation and to ensure the reliability of the power transmission network. It is commonly used to find the least-cost solution while satisfying all operational constraints, including line flow, bus voltages, generation constraints etc. Different objective functions have been selected in the optimization process, such as the total generation cost minimization, the social welfare maximization, and power loss minimization. However, minimizing the generation cost is the common objective function for power Utilities, Independent System Operators (ISOs), and Regional Transmission Organization (RTO). The optimization process includes equality constraints and inequality constraints. The equality constraints are the power balance equations between the generation and the load demands, and the inequality constraints are generation constraints, transmission line capacities etc. Although OPF provides relatively accurate results, it is not easy to take the system uncertainties into consideration.

The uncertainties in power system are caused by random variables, which are the load demands and renewable energy-based generation. Due to the adopted renewable portfolio standard (RPS), renewable energy resources, and particularly wind power, have been increasingly used by power companies to meet the load demand. Probabilistic optimal power flow (POPF) was proposed to deal with the stochastic uncertainties in power systems. In POPF, the random variables are represented by

probability distribution functions (PDF) based on the daily routine or historical data and are nonlinearly transformed (i.e. OPF) to obtain the distribution function of the output variables (e.g., voltage, line flows etc.).

The proposed POPF methods are classified into two categories: (i) simulation methods, and (ii) analytical methods. Monte Carlo Simulation (MCS) is the commonly used simulation approach in POPF. Numerous samples from different combinations of all the random input variables are transformed into the nonlinear system to get their corresponding outputs. This method gives results with acceptable accuracy. However, the large number of simulation cases makes the process time consuming and impractical for industry use. Nevertheless, due to its accuracy, MCS results are often used as the benchmark to compare and test the effectiveness of other analytical methods. In analytical methods, different algorithms are used to simplify the calculation and reduce the computational burden. However, most of them utilize linearization for power flow equations and lead to inaccurate results. Therefore, point estimation (PE) has been proposed to represent PDFs with fewer sample points. The results obtained from PE are within the acceptable accuracy range but it is not easy to handle the correlated random variables.

In this thesis, the unscented transformation (UT) is utilized to solve probabilistic optimal power flow (POPF). The proposed method has two advantages: (i) there is no need for linearization, and (ii) randomly distributed input variables (i.e., independent and correlated) and other system constraints are considered. Different UTs are simulated and tested on the IEEE 30- and 118-bus systems. The mean and standard deviation of locational marginal prices (LMPs) are compared to MCS method.

1.2.Contribution

The contribution of this thesis is two-fold: 1). the UT requires fewer sigma points to represent PDFs of the random variables. Therefore the computation burden associated with the POPF is reduced; 2). UT-based POPF results (e.g., voltage, power flows, etc) are more accurate since the sigma points, are selected through UT to represent PDFs of random variables and no linearization is used.

The proposed UT-based POPF algorithm is evaluated by simulating the effects of different random variables on the standard IEEE 30- and 118-bus power transmission systems. These two test cases represent a portion of the American Electric Power (AEP) transmission system in the Midwestern US. In this thesis, LMPs that are widely used by power Utilities to represent the electricity price in wholesale market, and to evaluate the performance of the UT-based POPF in different case studies.

Basic and General UT methods are applied with independent and correlated random variables and the results are compared to the corresponding MCS results. The mean and standard deviation errors are assessed with respect to wind farm locations and wind power penetration levels. Furthermore, performance of the method is evaluated for independent and correlated random variables.

1.3.Chapters Organizations

The thesis is structured as follows: Chapter 2 illustrates the POPF problem and the review of recent POPF literature, Chapter 3 presents UT and its application to POPF, and in Chapter 4, different simulation scenarios are presented based on the standard IEEE 30- and 118-bus system to demonstrate the effectiveness of the proposed algorithm. The proposed UT-based POPF algorithm results are discussed and compared with MCS for accuracy assessment. Lastly, Chapter 5 is the conclusion and proposed future work.

CHAPTER 2

POWER SYSTEM OPERATION

2.1. Introduction

Electric energy is not storable in large quantities and must be consumed immediately after it is generated, transmitted and distributed through an interconnected power grid. In order to achieve a reliable power system operation, continuous power balance between generation and load is required. Day-ahead, hour-ahead, and 5-minutes ahead generation scheduling are common practices by power grid operators to meet power supply and demand with the least-cost generation, and in regards to all operation constraints, line flows, voltage limits, generation constraints, etc. Increasing number of customers and uncertain power demands, combined with renewable energy-based generation proliferation adds more complexity to power system operation. Therefore, the probabilistic methods for power system analysis are needed to deal with the stochastic load and renewable generation.

This Chapter has four sections. First, the principles of power system and renewable energy integration are described. Then, power flow (PF) and optimal power flow (OPF) with their corresponding formulations, methods and characteristics are presented in Sections 2.3 and 2.4, respectively. Probabilistic optimal power flow (POPF) is reviewed in Section 2.5.

2.2. Power Systems and Renewable Energy Integration

Electric power is the essential element of any modern society. A power system is an interconnected large network that generates, transmits and distributes the electric power. The planning, operation and control of power system is becoming more important with the increasing load demand. The objective of a power system operation

is to supply electricity to all the customers continuously and reliably, while minimizing the total cost of generation.

A power system network is mainly divided into three sub-systems: the generation system, the transmission system and the distribution system [1]. Electricity is generated in generation plants using conventional resources, such as, coal and nuclear energy, or renewable energy resources, such as wind and solar power. After generated, electricity is boosted to a high voltage level by step-up transformers before it is transmitted over long distance in the transmission lines. The purpose of using high transmission voltage is to reduce the current and minimize power loss in form of heat, since power loss in the transmission lines is proportional to the square of the current ($P = I^2R$) [1]. Transmission lines deliver electricity to either transmission customers requiring high level voltage or regional substations that serve lower voltage customers. When electricity is transmitted to the end of the transmission system that is close to residential customers, step-down transformers are used to decrease the voltage and supply loads in the distribution system, as showing in Figure 1 [2].

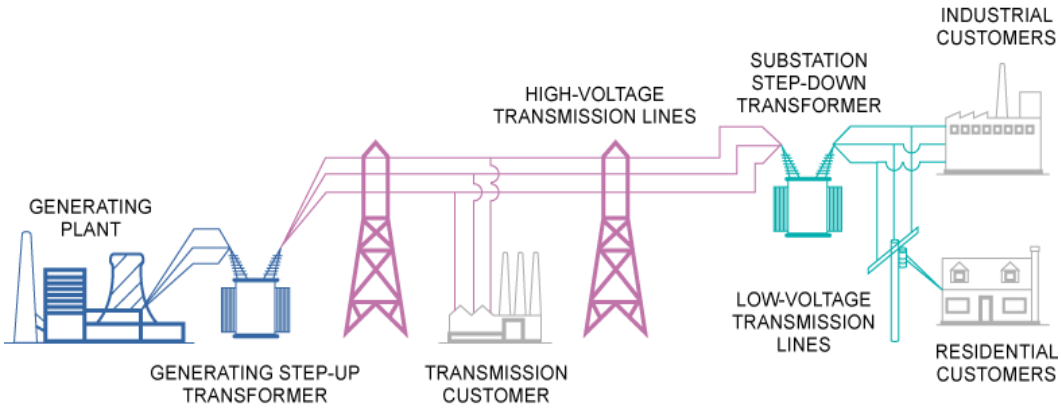

Figure 1. Power system network (Energy.gov, 2003)

Electricity cannot be stored in large amount. Once generated, it is transmitted to the end user at a speed of 200,000 kilometers per second. Therefore, accurate state forecasting is necessary to ensure system reliability and high quality electricity, before

power is transmitted. Steady state power flow is a fundamental and significant calculation to determine the bus voltage, generation and load conditions. The solutions are used in system planning and operation to ensure the power balance and system stability, i.e. the power generated should be equal to the load demands plus power loss [1].

In recent years, increasing amounts of renewable energy, especially wind power, has been integrated into the system [3]. Wind power is clean and does not generate greenhouse gases and air pollution, and is sustainable, unlike coal, oil and gas whose reserves are drastically decreasing. Wind power is particularly promising among current available renewable energy generation sources, the potential is enormous and the operation cost is decreasing. The price of wind power has decreased by over 80% since 1980, and some large wind turbines are capable of generating enough electricity to serve 600 homes [4]. All of these advantages make wind energy an attractive alternative power source in the long-run, especially in areas with less conventional energy sources.

Wind energy is already widely used in many countries. An increasing number of wind turbines has been built to provide electrical power in both developed and developing countries. In the United States, wind turbines are being built at a growing rate each year. In 2013, over 4% of the total electricity demand was provided by wind power and that number is rising rapidly [4]. According to the Department of Energy (DOE), 20% of the total electricity consumed in the U.S. will come from wind energy by 2030, and the number will increase to 35% by 2050. In China, wind power generation was over 150 billion kilowatt hours (kWh) and wind power capacity has reached 1360 GW by the end of 2014 [4].

Wind energy is considered as a promising alternative clean energy source all over the world. Wind power penetration has been greatly improved with refined wind turbine technology, as shown in Figure 2 [5]. In 2012, wind generation capacity increased to 60 GW globally, and wind power installation in the U. S was 90% higher compared to 2011. In 2013, wind power penetration increased by 269 MW in California and 61 GW were installed across 39 states [6].

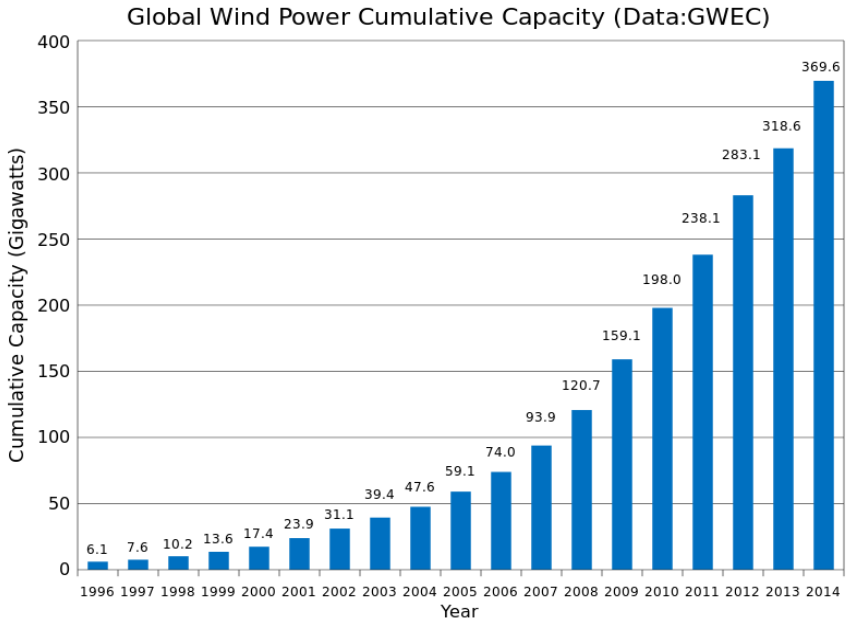

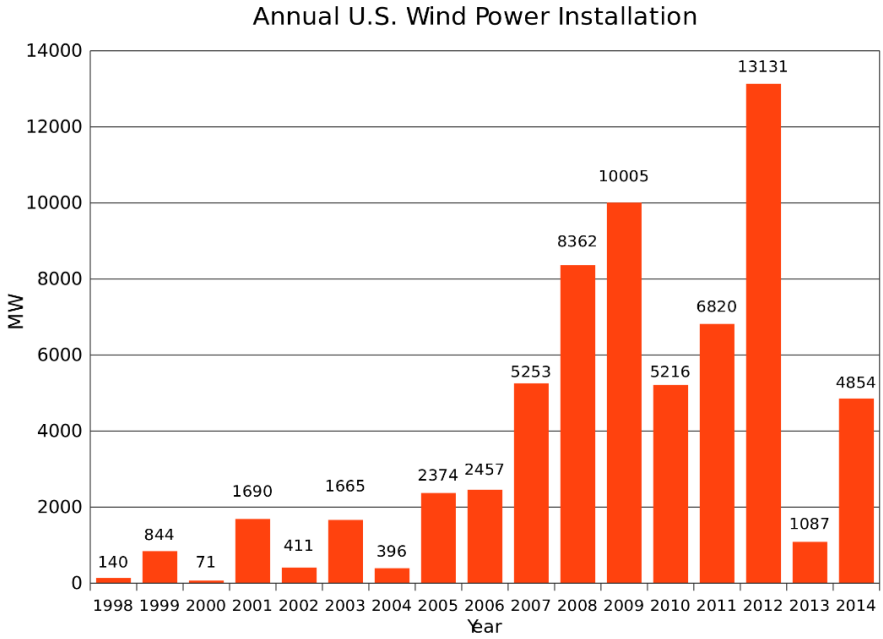

Figure 2 (a). Global wind power cumulative capacity (GWEC, 2011);

(b). Annual U.S. wind power installation (Delphi234, 2013)

Renewable energy-based generation proliferation complicates power system operation and planning due to the stochastic nature of the renewable energy [3]. It is difficult to calculate power system states when power system calculation process involves unspecified resources. The biggest challenge in using wind power is the instability due to its intermittent and fluctuation characteristics. Wind power integrated into the power system must be predicted regularly. In Midcontinent Independent System Operator (MISO), wind power forecasting is updated hourly, as shown in Figure 3 [7].

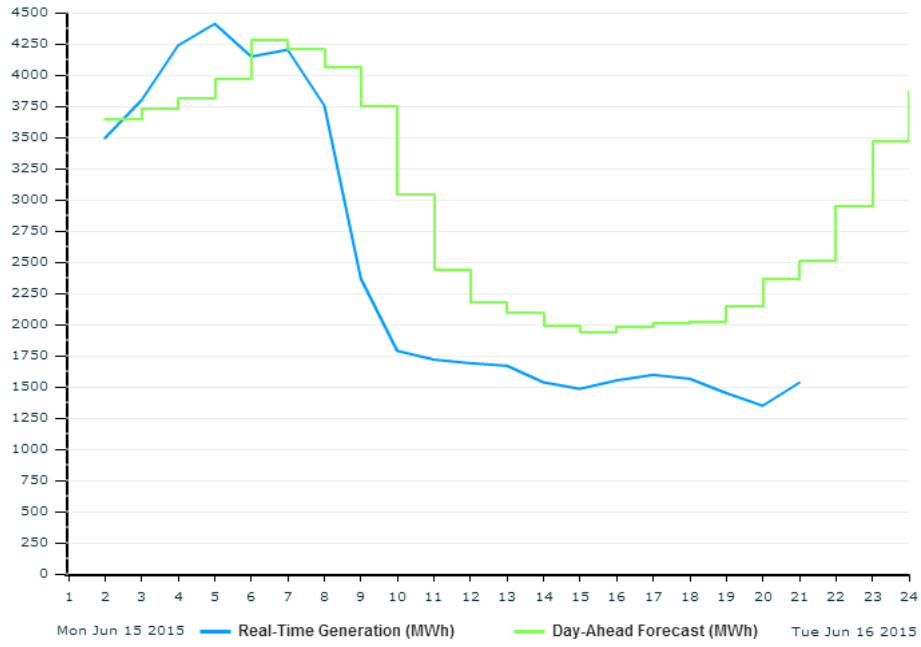

Figure 3. MISO day-ahead wind forecast (MISO, 2015)

2.3. Power Flow (PF)

To analyze the power system states, PF is widely used to determine the operating conditions for system planning and operation. PF is based on Kirchhoff's current law

and the power balance equations, which equate power generated to power consumed. According to Kirchhoff's current law, for each node in an electrical circuit, the sum of currents flowing into that node is equal to the sum of currents flowing out of that node. Combined with other power analysis equations, power balance equations are then formed to solve for the system states.

Power flow is the fundamental in determining how to operate the power system and how to plan its future expansion. The goal of PF is to establish steady-state operation conditions in a network and to ensure that the system is continuously reliable and secure to serve all customers. PF solutions are also used as the initial condition for other types of power system analysis, such as transient stability.

Each bus has four variables, voltage magnitude, voltage phase angle, real and reactive power. Two of the four variables are specified as the input variables to compute the other two unknown variables, using the power flow calculation [8]. All the buses in the network are categorized into three types: swing bus, or slack bus, voltage controlled (PV) bus and load (PQ) bus. The known variables in each bus is dependent on the type of the bus. Only one bus is selected as the slack bus, which works as the reference bus with known voltage magnitude and phase angle, i.e. $1.0\angle 0^{o}$. Real power (P) and voltage magnitude (V) are the known variables in PV buses. A bus with a generator or a switched shunt capacitors connected to it, is selected as the PV bus. In PQ buses, or load buses, real and reactive power are known, whereas the voltage magnitude and phase angle are unknowns. Once one bus is selected as the slack bus, other buses are either PV bus or PQ bus. Most of the buses within the power system are PQ buses [9].

PF equations are used to ensure the power balance at each bus in power grids. Before setting up power flow equations, the admittance matrix must be determined. In an n-

bus system, the admittance matrix Y is of size $n \times n$ and its entries are the equivalent circuit elements that model the system:

$$Y = \begin{bmatrix} Y_{11} & Y_{12} & \cdots & Y_{1n} \\ Y_{21} & Y_{22} & \cdots & Y_{2n} \\ \cdots & \cdots & \cdots & \cdots \\ Y_{n1} & Y_{n2} & \cdots & Y_{nn} \end{bmatrix} \tag{2.1}$$

Each diagonal element in the admittance matrix represents the admittance between a particular bus and all other buses connected to it. The off-diagonal elements represent the admittances between different buses. The admittance matrix is symmetric and its elements are given by the following equation [1]:

$$Y_{ij} = \begin{cases} y_{ii} + \sum_{k \neq i} y_{ik}, & if\ j = i \\ -y_{ij}, & if\ j \neq i \end{cases} \tag{2.2}$$

where y_{ij} is the admittance between two buses, and can be represented as $y_{ij} = g_{ij} + jb_{ij}$, g_{ij} is the conductance and b_{ij} is the susceptance.

Power flow equations are used to obtain the feasible solutions by balancing power between generators and customers. It is important to note that power loss is ignored in this study. Power flow equations are also used to solve for the unknown variables in the equations:

$$P_i = \sum_{k=1}^{n} |V_i||V_k|(G_{ik}cos\theta_{ik} + B_{ik}sin\theta_{ik}) \tag{2.3}$$

$$Q_i = \sum_{k=1}^{n} |V_i||V_k|(G_{ik}sin\theta_{ik} - B_{ik}cos\theta_{ik}) \tag{2.4}$$

where, P_i and Q_i are the injected real and reactive power at bus i, G_{ik} and B_{ik} are the real and imaginary parts of the admittance corresponding to the i_{th} row and k_{th} column in the Y bus matrix. θ_{ik} is the voltage angle difference between bus i and bus k.

There are two types of variables in the power flow study: the control variables and the state variables. Control variables include real power of the generators, voltage of

the generators, transformers tap setting, and inductance of the parallel elements. State variables are the bus voltage magnitudes and phase angles, non-controlled MV and MVAR of loads, fixed bus voltages, and line parameters. Once the control variables are specified, the state variables can be determined through power flow calculation. Feasible solutions from power flow problem can be applied as the initial conditions in solving other types of power system problems, such as fault location and contingency analysis.

Several methods are used to solve the nonlinear power flow calculation, among which Newton-Raphson is more often used. An initial solution is guessed and a series of successive approximations to the solutions are required in Newton-Raphson method. The "old" solution is updated and a "new" one is obtained that is closer to the correct solution in each iteration. The number of iteration in Newton-Raphson method is independent of the dimension, and the calculations converge in fewer than 10 iterations [10].

In Newton-Raphson's method, Jacobian matrix is formed,

$$J = \begin{bmatrix} \frac{\partial P_2}{\partial \delta_2} & \cdots & \frac{\partial P_2}{\partial \delta_n} & \frac{\partial P_2}{\partial V_2} & \cdots & \frac{\partial P_2}{\partial V_N} \\ \vdots & \cdots & \vdots & \vdots & \cdots & \vdots \\ \frac{\partial P_n}{\partial \delta_2} & \cdots & \frac{\partial P_n}{\partial \delta_n} & \frac{\partial P_n}{\partial V_2} & \cdots & \frac{\partial P_n}{\partial V_n} \\ \frac{\partial Q_2}{\partial \delta_2} & \cdots & \frac{\partial Q_2}{\partial \delta_n} & \frac{\partial Q_2}{\partial V_2} & \cdots & \frac{\partial Q_2}{\partial V_n} \\ \vdots & \cdots & \vdots & \vdots & \cdots & \vdots \\ \frac{\partial Q_n}{\partial \delta_2} & \cdots & \frac{\partial Q_n}{\partial \delta_n} & \frac{\partial Q_n}{\partial V_2} & \cdots & \frac{\partial Q_n}{\partial V_n} \end{bmatrix} \quad (2.5)$$

Where J, the Jacobian matrix is the partial derivatives of active and reactive power injection equations with respect to the state variables (i.e., voltage magnitude and angle). Steps for Newton-Raphson are as follows:

1. Set $x = \begin{bmatrix} \delta(i) \\ V(i) \end{bmatrix}$, and assume an initial solution $x^{(0)}$.

2. Determine the Jacobian matrix J
3. Solve the power flow equations to get $\Delta x^{(0)}$, $\begin{bmatrix}\Delta P\\ \Delta Q\end{bmatrix} = J * \Delta x$.
4. Check whether $\|\Delta x\| < \varepsilon$. If not, continue to the next step, otherwise the problem is solved.
5. Update the solution $x_{new} = x_{old} - \Delta x$, and go back to step 2.

ΔP and ΔQ are expressed by equations,

$$\Delta \mathrm{P} = -P_k + V_k \sum_{n=1}^{n} Y_{kn} V_n \cos(\delta_k - \delta_n - \theta_{kn}) \quad \text{k=2,3,…n.} \qquad (2.6)$$

$$\Delta \mathrm{Q} = -Q_k + V_k \sum_{n=1}^{n} Y_{kn} V_n \sin(\delta_k - \delta_n - \theta_{kn}) \quad \text{k=2,3,…n.} \qquad (2.7)$$

The iteration stops when all the mismatch are within the desired tolerance. Other assumptions and different algorithms are used to simplify the calculation, such as the utilization of the per-unit system.

In per-unit system, variables, such as voltage, current, power and impedance are expressed as per-unit quantities rather than their actual values. With the specified base quantities, power system can be simplified to the equivalent circuit. One of the most important advantages of per-unit system is that the ideal transformer winding is eliminated, and the transformer are replaced by equivalent impedances. There is no need to change the voltage, current or the other quantities referred to the other side of the transformers. Both the per-unit quantities and the elimination of the transformers significantly reduce power system calculation. Per-unit values of the parameters are defined as:

$$Per - unit\ Quantity = \frac{Actual\ Quantity}{Base\ Value\ of\ the\ Quantity} \qquad (2.8)$$

where, the actual quantity is the variables in actual unit, the base value is a real number used as the reference to compute the per-unit quantity. Since both actual and base quantities are real numbers, voltage angle is the same as the angle of the actual quantity

in per-unit system [10]. The commonly used parameters are the impedance, voltage and current. The per-unit system can be used in both single phase and three phase power systems. Based on the definition, in single phase system, per-unit quantities are:

$$V_{pu} = \frac{V}{V_{base}} \tag{2.9}$$

$$I_{pu} = \frac{I}{I_{base}} \tag{2.10}$$

$$S_{pu} = \frac{S}{S_{base}} \tag{2.11}$$

$$Z_{pu} = \frac{Z}{Z_{base}} \tag{2.12}$$

Once two of the variables are established, then the other two variables can be determined from the following equations.

$$I_{base} = \frac{S_{base}}{V_{base}} \tag{2.13}$$

$$Z_{base} = \frac{V_{base}}{I_{base}} = \frac{V_{base}^2}{S_{base}} \tag{2.14}$$

Voltage magnitude V and complex power S are usually selected as the base variables because voltage value does not deviate significantly from rated value when the loads change, and the power quantity is related to the voltage, which is also expected to be in a given range. In addition, base complex power is the same for the entire power system and the impedance remains the same when referred from one side of the transformer to the other side [10].

Power system problems can be challenging when system constraints or limitations are taken into account. There are numerous constraints in the system, such as bus voltage, generation power and transmission line limitations. Various hypothetical conditions are made in order to simplify the problem. In most cases, the system is assumed to be in steady state and the frequency is assumed to be constant. Other assumptions are used either to make the problem close to practical conditions or to

simplify calculations. However, to ensure power system security and stability, uncertainties resulting from loads fluctuation and un-dispatchable renewable energy sources must be taken into account when determining the operation states.

2.4 Optimal Power Flow (OPF)

Optimal power flow (OPF) was first proposed by Carpentier in 1962, and now becoming widely used by power system operators to analysis power systems. In OPF, system constraints, such as the transmission line limitations, power distribution range from the generators and load changes are taken into account to give optimal and more practical solutions.

One objective function is created and need to be optimized in OPF. The objective function has various forms, such as total generation cost, total transmission losses or reactive source allocation. For power utilities, minimization of the total generation cost is commonly used as the objective function. The optimization calculation in OPF helps to obtain the optimal solutions to operate the system while ensuring its security and reliability. Both equality and inequality constraint are taken into account in OPF calculation.

Inequality constraints represent the limitations of the generators and the transmission lines of the system. For example, the voltage of each bus must remain in a specific range:

$$V_{imin} \leq V_i \leq \mathrm{V_{imax}} \tag{2.15}$$

The real power of the transmission line must remain in a prescribed range:

$$P_{lmin} \leq P_l \leq P_{lmax} \tag{2.16}$$

The real and reactive power of the generator must be limited to its rating:

$$P_{Gmin} \leq P_G \leq P_{Gmax} \tag{2.17}$$

$$Q_{Gmin} \leq Q_G \leq Q_{Gmax} \tag{2.18}$$

Several methods and optimization techniques have been proposed to solve the OPF. The primary methods in power flow calculation are generally classified into two types: conventional methods and intelligent methods. Conventional Methods include: linear programming, gradient algorithms, Newton's method, quadratic programming, and interior point algorithms. All these methods have long been used to effectively solve OPF.

The reduced gradient method was proposed by Dommel and Tinney in 1968 [1]. Newton's method was then introduced and widely used because of its fast convergence rate. Lagrange techniques combined with the necessary conditions (Kuhn-Tucker condition) are used in these methods to minimize the objective function. This technique is effectively used in dealing with the constraints to linearize the problem. Although many intelligent methods such as, genetic algorithms, artificial neural network and particle swarm optimization have been recently studied, the classical methods are still used in solving the OPF. The reduced gradient method converges fast, but the speed of convergence is greatly influenced by the value of the step factor. The number of iteration increases if the value of the variable is too small, and causes fluctuations about the optimal solution if the value is too high. The limitation in gradient method is that the oscillation phenomena cannot be avoid completely [36].

In order to minimize the objective function, subject to the constraints, the gradient of Lagrange function is set to be zero in Newton's method. The necessary condition to minimize the cost function is to set the derivative of the function with respect to the state variables to be zero, which is $\nabla \mathcal{L} = 0$. Initial condition is set and updated in the

nonlinear process to obtain the optimal solution, through iteration calculation based on the following equations:

$$\mathcal{L}(x, \mu, \lambda) = f(x) + \mu^T h(x) + \lambda^T g(x) \tag{2.19}$$

$$\nabla^2 \mathcal{L}\left(x^{(k)}\right) * \Delta x(k) = -\nabla \mathcal{L}\left(x^{(k)}\right) \tag{2.20}$$

$$\Delta x(k) = -\nabla \mathcal{L}\left(x^{(k)}\right) * \left[\nabla^2 \mathcal{L}\left(x^{(k)}\right)\right]^{-1} = -\left[\mathrm{H}\left(x^{(k)}\right)\right]^{-1} * \nabla \mathcal{L}(x^{(k)}) \tag{2.21}$$

$$x^{(k+1)} = x^{(k)} + \Delta x^{(k)} \tag{2.22}$$

where $\mathcal{L}$ is the Lagrange function, *f* is the objective function, *h* and *g* are the equality and inequality constraints. x is the state vector and, μ and λ are the Lagrange coefficients. *k* is the order of the iteration. The second order of partial derivative with respect to the state variables is called Hessian (H) matrix. Jacobian and Hessian matrix used in OPF are represented by the following matrix:

$$J(x) = \begin{bmatrix} \frac{\partial f_1(x)}{\partial x_1} & \frac{\partial f_1(x)}{\partial x_2} & \cdots & \frac{\partial f_1(x)}{\partial x_n} \\ \frac{\partial f_2(x)}{\partial x_1} & \frac{\partial f_2(x)}{\partial x_2} & \cdots & \frac{\partial f_2(x)}{\partial x_n} \\ \vdots & \ddots & \ddots & \vdots \\ \frac{\partial f_n(x)}{\partial x_1} & \frac{\partial f_n(x)}{\partial x_2} & \cdots & \frac{\partial f_n(x)}{\partial x_n} \end{bmatrix} \tag{2.23}$$

$$H(x) = \nabla^2 \mathcal{L}(x) = \begin{bmatrix} \frac{\partial^2 \mathcal{L}}{\partial x_i \partial x_j} & \frac{\partial^2 \mathcal{L}}{\partial x_i \partial \mu_j} & \frac{\partial^2 \mathcal{L}}{\partial x_i \partial \lambda_j} \\ \frac{\partial^2 \mathcal{L}}{\partial \mu_i \partial x_j} & 0 & 0 \\ \frac{\partial^2 \mathcal{L}}{\partial \lambda_i \partial x_j} & 0 & 0 \end{bmatrix} \tag{2.24}$$

The feasible solution is updated in the iterative process until the variables are within their specified tolerance. Newton's method has been widely used for decades to solve OPF. The disadvantages of these methods are that they converge slowly and may get stuck at a local optimum, which makes them difficult to use in large-scale system.

The standard procedure for solving OPF is to create the bus admittance matrix based on the network parameters, and to make initial estimation of the voltage at each bus. Solutions are determined by substituting the initial conditions into the power flow

equations and iterating the process. The estimated voltages are updated according to the corresponding numerical algorithms. This process is repeated until the tolerances are within acceptable ranges. In practice, OPF is used by power companies to calculate the state variables to operate the system and determine the electricity price in different locations. These voltage magnitudes, angles and locational electricity price are used to obtain assess predict the working operating condition of conditions for the existing system or for the future transmission system expansion plans prediction.

Intelligent Evolutionary-based OPF methods include the genetic algorithms, artificial neural network, particle swarm optimization, and colony algorithms. Compared to the conventional methods, intelligent evolutionary-based methods can find multiple optimal solutions in a single run much faster. Also, it is easy to get the global optimal solution using intelligent such methods. However, there are some disadvantages to intelligent method, such as their large dimensionality and the computational burden.

By guessing the initial OPF solution and evaluating the inequality constraints, solution is updated until the acceptable error is satisfied. OPF solution minimizes the total generation cost while meeting the power system demands, ensuring that all the constraints are within their desired operation ranges, and maintaining the system security. OPF is capable of determining the locational marginal price that includes the transactions and auxiliary service cost, and widely used by power utilities [10]. OPF calculation has many applications in power system, such as real-time control, operational planning, and other areas in modern EMS.

The OPF can be used regularly (every five minutes) to find the optimal operation state for the system, including the voltage and reactive power of generators and transformer tap position. The electricity market enables to balance the supply and

demand and set the price to purchase and sale electricity effectively. The operators are required to ensure the reliability and efficiency of the system. In the competitive electricity market, it is critical to evaluate power system states and establish a sustainable electrical power cost. The electricity price function should reflect the real-time cost regulation. In order to meet the demands of the electricity market, powerful OPF tools with high convergence speed are required to accurately estimate the continuous cost of running the generators and meet the operation requirements during the worst conditions. Currently, OPF estimation is one of the most important methods in electricity market with frequent changes in bid and offer.

In OPF formulation, optimal solutions can be established and the security of the system can be ensured by setting the controllable variables (e.g., power generation, voltage set point) within a specified range [1]. However, when some of the variables in the formulation are randomly distributed, it is not easy to predict all the possible distributions and optimize system operation.

2.5. Probabilistic Optimal Power Flow

Probabilistic optimal power flow (POPF) was proposed by Borkowska in 1974 to determine the statistical characteristics of the output variables considering the random input variables [6]. All the random variables are represented by their probability distribution functions derived from the history data or reasonable assumptions. The random variables are assumed to be mutually independent. Statistical characteristics of the corresponding output variables are determined by running the optimal power flow. Various values of the random input variables, such as the voltages at all buses and the power flow of the transmission lines, are converted into power flow equations to obtain the corresponding states of the output variables. In this thesis, random variables are the

loads and wind power. These variables are assumed to be normally distributed and are nonlinearly transformed to determine the output variables. Analyzing the statistics of the optimal power flow results, PDFs of the output variables are obtained [11-12].

In practice, the system variables are not easy to forecast due to many reasons, such as random load fluctuations. Also, with renewable power sources integrated into the system, such as hydro, solar, and wind, the system can become unstable and their stochastic nature need to be taken into consideration [1]. Particularly, in recent decades the capacity of wind power generating has increased significantly due to increasing number of wind farms built. As a result of the stochastic characteristics of wind power, power systems are becoming more uncertain with the increasing wind power penetration [13]. For system planning and forecasting related to the operation states, uncertainties from both loads and wind power should be considered to ensure the system stability and reliability.

Probabilistic optimal power flow (POPF) was proposed to solve the OPF problem, while representing the random variables using the probability distribution function. PF with a specific objective function and adjustable variables forms the POPF problem. POPF methods compute the random input variables, represented by their PDFs, to obtain the characteristics of the output variables, such as power loss, LMP and power generation, which are also random variables with probability density functions. Unlike OPF, POPF includes random variables with known PDFs. In system with uncertainties from loads or renewable energy, POPF is more accurate in simulating the system. This is convenient to get all the possible results of power flow within specific ranges. By using PDF, all combinations of possible values within a given range of loads and generators can be computed.

Numerous methods have been proposed to solve the POPF including simulation methods and linearization methods [8]. To ensure system reliability, different variables should be controlled in a specified range. However, system outputs depend on the input variables, and different characteristics of the input variables will lead to different results. In order to predict system states accurately, all possible combinations of the input variables need to be taken into account. Large numbers of possible output are generated according to the various random input variables. Given all the possible combinations of the input variables and the large number of buses in a practical network, the calculation can get extremely complicated. Furthermore, the power flow transformation computation process is complex due to the nonlinear equations. The calculation steps and time can be enormous and impractical. One of the methods to reduce the calculation load is to select specific values of loads around their mean value, which yields a precise output within a short time.

Without a particular way to predict the states of all the random variables, the accuracy of the results depends on the applied algorithms. However, the accuracy of the results is still not reliable and needs to be improved.

2.5.1. Probability Distribution Functions (PDF)

In a mathematic model, the values of the random variables are represented by PDFs. For a continuous random variable, the PDF is a function describing the relative likelihood of the random variable to take a given value [12]. It is expressed as the integral of the variable's density between two boundary limits (or the area below):

$$P(a < x < b) = \int_a^b f_X(x)dx \tag{2.25}$$

where, P is the integral distribution function and f (x) is the probability density function. PDF properties include:

$$\int_{-\infty}^{\infty} f_X(x)dx = 1 \quad (2.26)$$

$$f_X(x) \geq 0, \forall x \quad (2.27)$$

$$f_X(x) = \frac{dF_X(x)}{dx} \quad F_X \text{ is the cumulative distribution function of x} \quad (2.28)$$

To represent the random variables, PDFs with known properties are used to describe and predict the values of input random variables. To represent the uncertainty in loads, expected values and their deviation are estimated based on the distribution functions. Based on a typical PDF algorithm, fixed values of the loads, generations and other parameters with expected values are used in the power flow equations to estimate power flow and other variables.

2.5.2. Probabilistic Optimal Power Flow Formulation

Although the loads and wind power are random variables, they still change in a certain range that can be determined. It is assumed that the expected outputs of these uncertain variables originate from the historical data and vary within specific ranges. Variables are then represented by PDFs, and the parameters in the functions are determined from past datasets. The standard function for the probability power flow is:

$$Y = f(X) \quad (2.29)$$

$$Z = g(X) \quad (2.30)$$

where, Y is the input power vector for the buses, X is the state random vector, Z is the output line flow vector, and f and g are the nonlinear power flow equations and power injections involved. Once the power injections are determined, state variables can be established and line flow values can also be obtained.

2.5.3. Probabilistic Optimal Power Flow Methods

The main issue regarding POPF is to obtain the statistical moments or PDFs of the output of a nonlinear system having random input variables. Several methods have been proposed to solve the POPF problem, and the methods are categorized into two types:

simulation methods and analytical methods. Analytical methods use mathematical solutions to assess the system performance, and simulation methods evaluate the system by running PF with adequate input variable combinations.

2.5.3.1. Monte Carlo Simulation

The commonly used simulation method is the Monte Carlo Simulation (MCS). MCS is a straightforward computational method mainly used in optimization, numerical integration and generation draws from probability distributions [14]. Input variables are pseudo random numbers generated according to a distribution function. Random samples carrying properties of specified distributions are the utilized as the input and simulated in MCS to obtain the consistent results. Numerous simulation results are then obtained based on the different input combinations. By analyzing the properties of the outcomes statistically, the statistical parameters of the output variables are obtained. The number of simulations depends on the size of the system. MCS is a stochastic process that is commonly used in power system evaluations.

MCS is extremely useful in multidimensional integration and simulation of stochastic natural phenomena.

The advantages of using MCS methods are:

1. Free from the restrictions of solving Newton's equation of motion.
2. Faster and efficient.
3. Easily parallelizable.
4. Independent of dimension, according to central limit theorem, the variance of the integrand is finite. Approximately useful for dimension >8.

MCS directly solves the POPF by generating different combinations of input variables. The PDF of the input variables are usually assumed to be normally distributed

and represented by pseudo-random numbers. The method directly uses non-linear power flow equations and provides highly accurate results by using a large number of simulations. However, the numerous simulations make it costly, time-consuming, and impractical, especially for large power networks. It is not easy to find a balance between statistical error and systematic errors. Because of its accuracy, MCS is widely used as the standard to test the effectiveness and accuracy of other proposed methods.

2.5.3.2. Linearization Methods

Solving POPF is so complex that no simple algorithm can be used to get the solution. In large power system network with larger number of buses, more work is needed for the analysis. In order to reduce the computation load, various analytical methods are proposed to approximate the solution. Assumptions are made to simplify the complex calculation from the non-linear power flow equations and the uncertainty of the input variables. Linearization is commonly used in various methods to simplify the system by linearizing power flow equations around the expected range. Power flow equations are linearized by using a first-order approximation of the Taylor expansion. Distribution functions of the input random variables are linearly transformed to determine the distribution functions of the output variables.

2.5.3.3. Convolution Method

Let X and Y be two independent discrete random variables with probability density functions f_x andf_y. If

$$Z = X + Y \tag{2.31}$$

Then the distribution function of Z, f_Z, can be determined as:

$$f_z(z) = \int_{-\infty}^{\infty} f_X(z-y) f_Y(y) dy \tag{2.32}$$

This operation is called the convolution. If M is the sample sum of the independent random variables $X_i, i = 1,2, \dots, n$, with different density function $f_i, i = 1,2, \dots, n$, respectively, then the probability distribution function of M is the convolution of all the pdfs:

$$f_m = f_1 * f_2 * \dots * f_n \tag{2.33}$$

Independent random variables can be combined to form new random variables through addition with suitable coefficients. In [15], a convolution method is applied to obtain the pdf of the sum of independent input variables. In [16], numerous inputs satisfying the system constraints are selected to simulate the system in order to improve the accuracy. Any value can be used as the input as long as they are within the boundaries of the constraints. Setting boundary limits simplifies the selection of input variables, however, the boundary algorithm can lead to slow and difficult convergence.

The convolution method can handle independent random variables that are linearly related and help reduce the computation load, however it is not simple to determine the PDFs of all the power injections. The Fast Fourier Transform (FFT) based on the convolution property was proposed in [15-16]. FFT based convolution algorithm is applied to implement the impulse process from the convolution by determining and separating the boundaries of the functions. Points in different regions are selected as the input values to estimate the states of the system. The FFT takes advantage of the exponential function properties, which makes the calculation faster and more accurate.

2.5.3.4. Moment and Cumulant Method

Taylor expansion includes a series of moments that can help identify the probability distribution of a random variable. The first moment of X, μ_1 or $E(X)$, is also called the mean or expected value of a random variable X,

$$\mu_1 = E(X) = \int_{-\infty}^{\infty} xf(x)dx \tag{2.34}$$

Higher moments of X is μ_r or $E(X^n)$, n>1, and expressed by

$$\mu_r = E(X^n) = \int_{-\infty}^{\infty} x^n f(x)dx \tag{2.35}$$

The moments of a population are estimated by sample moments. Properties of moments are:

1. $E(c) = c$, c is a constant. (2.36)
2. $E[aX + b] = aE[X] + b$, a and b are constants. (2.37)
3. $var(X) = E[(X - x)^2] = E(X^2) - [E(X)]^2$, x is the mean value. (2.38)
4. $var(aX + b) = a^2 var(X)$. (2.39)

The cumulate function is the Laplace transform of a probability distribution. It can completely characterize the probability distribution due to the uniqueness of Laplace transformation. The cumulate algorithm requires less computation compared to the convolution computation.

The moment generating function, based on equation defining the moments, is given by

$$F(\theta) = E\left(e^{\theta X}\right) = E\left(1 + \theta X + \cdots + \frac{\theta^r X^n}{n!} + \cdots\right)$$

$$= \sum_{n=0}^{\infty} \mu_r \frac{\theta^r}{n!} \tag{2.40}$$

$$K(\theta) = logF(\theta) = \sum_r k_r \frac{\theta^n}{n!} \tag{2.41}$$

The cumulants k_r are the coefficients in the Taylor expansion of the cumulant generation function.

The relation between the first few moments and cumulant can be obtained by extracting coefficients from the expansion as following

$$k_1 = \mu_1 \tag{2.42}$$

$$k_2 = \mu_2 - {\mu_1}^2 \tag{2.43}$$

$$k_3 = \mu_3 - 3\mu_2{\mu_1}^2 + 2{\mu_1}^3 \quad (2.44)$$

$$k_4 = \mu_4 - 4\mu_3\mu_1 - 3{\mu_2}^2 + 12\mu_2{\mu_1}^2 - 6{\mu_1}^4 \quad (2.45)$$

Alternatively, we use the reverse direction

$$\mu_2 = k_2 + {k_1}^2 \quad (2.46)$$

$$\mu_3 = k_3 + 3k_2{k_1}^2 + {k_1}^3 \quad (2.47)$$

$$\mu_4 = k_4 + 4k_3k_1 + 3{k_2}^2 + 6k_2{k_1}^2 + {k_1}^4 \quad (2.48)$$

where, $k_1 = \mu_1$ is the mean of X, k_2 is the variance.

The cumulate is a nonlinear combination of moments obtained from the cumulant generating function. The cumulants of a probability distribution are a set of quantities providing an alternative to the moments of the distribution.

After linearization, cumulates are obtained by solving the equations in each order, and the random variables are then replaced by a combination of their cumulants. In [17], Hermite Polynomial expansion was proposed, to take advantage of the relationship between the moments and cumulates simplifying the distribution function. Corresponding cumulants are added to get convolved cumulants. Convergence problem can be solved by standardizing the process based on least square error. Cumulants are applied to independent random variables instead of moments for the following reasons:

1. Cumulants accept any random variables.
2. The cumulants of a sum are the sum of cumulants.
3. Cross cumulants are zero.
4. Other methods are easily applied based on cumulants.

2.5.3.5. Gram-Charlier Method

Gram-Chalier approximates a probability distribution in terms of its cumulants. The main concept in the expansion is to express the distribution based on the characteristic

distribution with known properties. In addition to the first and second moments that describe the distribution function, Gram-Charlier expansion introduces the third and fourth (skewness and kurtosis) moments as additional parameters to improve the accuracy. For random variables that are assumed to be normally distributed, their PDF can be approximated as

$$g(z) = P_n(z)\varphi(z) \tag{2.49}$$

where $\varphi(z)$ is the standard normal distribution density and $P_n(z)$ is used to ensure that $g(z)$ has the same first moments as the PDF of z. $P_n(z)$ is approximated using

$$P_n(z) = \sum_{i=0}^{n} c_i He_i(z) \tag{2.50}$$

where $He_i(z)$ are the Hermit polynomials. The i^{th} order Hermit polynomial is $He_i(z) = (-1)^i(\partial^i\varphi/\partial z^i)/\varphi(z)$. The standardized z has the following properties:

$$\int_{-\infty}^{\infty} zg(z)dz = 0 \tag{2.51}$$

$$\int_{-\infty}^{\infty} z^2 g(z)dz = 1 \tag{2.52}$$

$$\int_{-\infty}^{\infty} z^3 g(z)dz = \gamma_1 \tag{2.53}$$

$$\int_{-\infty}^{\infty} z^4 g(z)dz = 3 + \gamma_2 \tag{2.54}$$

The multivariate Gram-Charlier series (GCS) was proposed to represent the PDF of independent randomly distributed variables. The Gram-Charlier series approximates the probability distribution function. After computing the GCS, the PDF is then formed to represent the skewness, kurtosis and other high order coefficients [18-19].

With GCS, PDFs can be described using a finite number of terms. The precision of GCS can be extended up to the fifth order term, and convergence is faster when the approximate vector uses standard normal distribution and the respective derivatives. Other algorithms have been proposed to determine the Gram-Charlier expansion coefficients. Among these algorithms, the cumulant process was used based on the fact

that the inverse of Hessian is the logarithmic barrier of interior point linear mapping [18]. The cumulative distribution function and probabilistic distribution function of a normalized variable can be expressed as a series of standard normal distribution and their respective derivatives. A linear function is formed by combining the cumulants of random variables, however, this is not accurate in higher level uncertain systems.

2.5.3.6. Cornish-Fisher Method

In Cornish-fisher method, the effects of skewness, kurtosis and higher moments in expanding the distribution function are taken into account. Cornish-fisher expansion is a formula that represents the random variable based on its first few cumulants. Cornish-fisher expansion transforms a standard Gaussian random variable into non-Gaussian random variable.

The mean and standard deviation of a standard normally distributed variable X are 0 and 1, and the expansion to approximate the q-quantile based on its cumulants is $\Phi_X^{-1}(q)$. Considering the first five cumulants, the expansion is expressed as [20-21]:

$$\begin{aligned}\Phi_X^{-1}(q) \approx \Phi_Z^{-1}(q) &+ \frac{\Phi_Z^{-1}(q)^2-1}{6}\kappa_3 + \frac{\Phi_Z^{-1}(q)^3-3\Phi_Z^{-1}(q)}{24}\kappa_4 \\ &- \frac{2\Phi_Z^{-1}(q)^3-5\Phi_Z^{-1}(q)}{36}\kappa_3^2 + \frac{\Phi_Z^{-1}(q)^4-6\Phi_Z^{-1}(q)^2+3}{120}\kappa_5 \\ &- \frac{\Phi_Z^{-1}(q)^4-5\Phi_Z^{-1}(q)^2+2}{24}\kappa_3\kappa_4 + \frac{12\Phi_Z^{-1}(q)^4-53\Phi_Z^{-1}(q)^2+17}{324}\kappa_3^3\end{aligned} \tag{2.55}$$

In [19], Cornish-fisher expansion only uses the first 5 cumulants and reaches convergence by estimating CDF (cumulative distribution function). Unlike the Taylor series expansion which truncates at a specific point, Cornish-fisher use all terms. Regardless of the length of the expansion, using more than five cumulants does not necessarily produce better approximation. In Cornish-fisher expansion, the q-quantile

of a cumulative distribution is approximated in terms of the quantile of a normal distribution and the cumulants of the cumulantive distribution function.

Although the variables in Cornish-fisher are required to have a standard normal distribution, quantiles of other variables can be approximated by normalization. If the mean and standard deviation of variable X is μ and σ, X can be standardized using the equation:

$$X^* = \frac{X-\mu}{\sigma} \tag{2.56}$$

to have mean 0 and standard deviation of 1. Also the central moments of X^* can be expressed using:

$$\mu_r^* = \frac{\mu_r}{\sigma^r} \tag{2.57}$$

By applying the Cornish-Fisher expansion to determine the q-quantile $x^*$of X^*, q-quantile x of X is calculated as

$$x = x^*\sigma + \mu \tag{2.58}$$

Through the central moments of normalized random variables, q-quantiles of random variables can be determined. However, all linearization methods transform the points from the distribution function inaccurately, especially in the tail region. Besides, the linearization of uncertain input variables can lead to inaccurate transformation especially for variables with high level of uncertainty.

The discussion above shows the effectiveness of more accurate method in handling the random variables. However, the linearization in these methods requires a Jacobian matrix, which increases the computational load and errors. Also, some of the linearization methods do not take into account the correlation between the variables. In power systems, different loads or generators are correlated. The loads are mutually

correlated because of environmental and social factors. In some areas wind farms are affected by similar factors and perform with similar characteristics.

2.5.3.7. Point Estimation Method

Point estimation (PE) is another method in solving the POPF. PE estimates the parameters of a probability distribution function based on the data observed. Expected points are determined by linearization to represent the normal distribution functions.

Several PE methods are used to analyze the stochastic process, such as Hong's, Lin's and Harr's [22]. Among these methods, Hong's point estimation method is the most effective since it can handle multiple random variables without increasing the computational load. For example, the original 2PE method with n variables will run for 2^{n} times to generate results, whereas, Hong's method will generate accurate results in 2n runs. The method uses only the first three moments of the distribution function, which reduces the computational load without compromising the accuracy of the results.

The main concept of the point estimation method is to evaluate the function (F) several times for each variable P_l. $P_{l,k}$ is the k^{th} value of P_l. evaluated.

$$F = (\mu_{p1}, \mu_{p2,} \dots p_{l,k}, \dots, \mu_{pn}) \tag{2.59}$$

Each of the variables, P_l will be evaluated k times. Then the function is determined using the mean of other input variables. The total calculation runs is $k * n$.

Juan. M. Morales, and Juan. Pérez-Ruiz's paper utilized Hong's PEM as [23]:

$$P_{l,k} = \mu_{P_l} + \xi_{l,k}\sigma_{P_l} \tag{2.60}$$

$\mu_{pl}\ and\ \sigma_{pl}$ are the mean and standard deviation of f_{pl}. Parameter $\varepsilon_{l,k}$ is from the equation:

$$\xi_{l,k} = \lambda_{l,3}/2 + (-1)^{3-k} * \sqrt{m + (\lambda_{l.3}/2)^2} \tag{2.61}$$

This can be applied when k=1 and 2.

$$\lambda_{l,3} = \frac{E[(P_l - \mu_{P_l})^3]}{(\sigma_{P_l})^3} \tag{2.62}$$

where, $E\left[\left(P_l - \mu_{P_l}\right)^3\right] = \sum_{t=1}^{N}(P_{l,t} - \mu_{P_l})^3 * Prob(P_{l,t})$.

The weights are from

$$w_{l,k} = \frac{1}{n}(-1)^k \frac{\xi_{l,3-k}}{\zeta_l} \tag{2.63}$$

where $\zeta = 2\sqrt{m + (\lambda_{l.3}/2)^2}$. $\xi_{l,k}$ is the standard location of the variable. The weight (w) is established using

$$\sum_{k=1}^{K} w_{l,k} = \frac{1}{m} \tag{2.64}$$

$$\sum_{k=1}^{K} w_{l,k}(\xi_{l,k})^j = \lambda_{l,j} \qquad j = 1, \ldots 2K-1 \tag{2.65}$$

where the standard central moment $\lambda_{l,j}$ is

$$\lambda_{l,j} = \frac{M_j(P_l)}{(\sigma_{P_l})^j} \tag{2.66}$$

$$M_j(P_l) = \int_{-\infty}^{\infty}(P_l - \mu_{P_l})^j f_{P_l} d_{P_l} \tag{2.67}$$

After generating all the $P_{l,k}$ and the $w_{l,k}$ values, the function F is determined to calculate the results for $Z_{l,k}$. The moment of the output variable is

$$\mu_j' = E[Z^j] \cong \sum_{l=1}^{m}\sum_{k=1}^{K} w_{l,k}(Z(l,k))^j \tag{2.68}$$

When $k = 2$, then 2n calculations are used to get the output.

Chun-Lien Su used the two point estimation method to obtain the uncertainty [22]. In their study, P_l is also the random variable from the PDF f_{P_l}. Two P_l variables $P_{l,1}$ and $P_{l,2}$ replace the f_{P_l} following the equation:

In [22], point estimation through orthogonal transformation solved the dependent variables, such as load demands. With fewer moments, the first 4 concentration points are established. Each point determines three evaluations, and the total number of calculations with m variables is $2m + 1$. The results are compared with MCS to

evaluate the effectiveness and accuracy of the method even with high wind power generation.

Point estimation [22-23] can solve multiple random variables without increasing the computing load. With only $2n$ points, results with acceptable accuracy can be achieved. However, it is not easy to deal with correlated random variables using PE method.

2.6. Locational Marginal Price (LMP)

In electricity market, OPF solution is extremely important in solving the power system challenges, such as the economic dispatch. OPF is utilized in the pricing mechanism to rationally fix the cost of the power system. Independent system operators (ISOs) need to apply OPF to manage power market intelligently in order to maintain the balance between generation and demands. In the real-time and day-ahead market, price of the system has to be forecasted in competitive power market.

Several constraints are considered in the formulation, such as the limitations from the loads, generators and transmission lines. Utilities establish the locational marginal price (LMP), or the nodal price, by solving the OPF problem. LMP is the cost to supply the next megawatt (MW) of electricity at a particular location in consideration of all constraints [8]. The node price is the cost of power increased by 1MW. It is composed of three elements: the cost to produce energy, congestion cost due to the constraints, and the cost of losses. Without system constraints and losses, the price of electricity at all buses would be the same. However, when all the factors are considered, the price to serve the loads varies in different locations.

LMP is the result of economic dispatch and is used in electricity market to price electricity. LMP is calculated at each load zone for the external interface. By

considering the different prices of serving electricity in different areas, the energy source at lower cost is first used to meet the loads. Other nearby generators are then used to satisfy the remaining load demand subject to the transmission conditions. The states of the system, considering the uncertainties, are manifested by the electricity prices in different locations.

LMP is one of the commonly used parameters to indicate the precision of the POPF algorithms. The parameters reflect the impact of a node on the stability problem, which can also be used to determine the apportioning electricity among market participants. By using the method of probabilistic optimal power flow, we can minimize the generations cost and improve the reliability. The optimal solution can then be used to determine the price and the amount of electricity to be generated in order to meet the demands of the different types of clients.

In a real-world power system, transmission line constraints ensure the safety and reliability of the system. An independent system operator (ISO) calculates the LMPs for the real-time and day-ahead market to determine the price of electricity for the wholesale market and the transmission costs, as described in Figure 4 [24]. In practice, OPF is utilized by ISO, such as MISO and California ISO, to regulate electricity for wholesale day-ahead or real-time market.

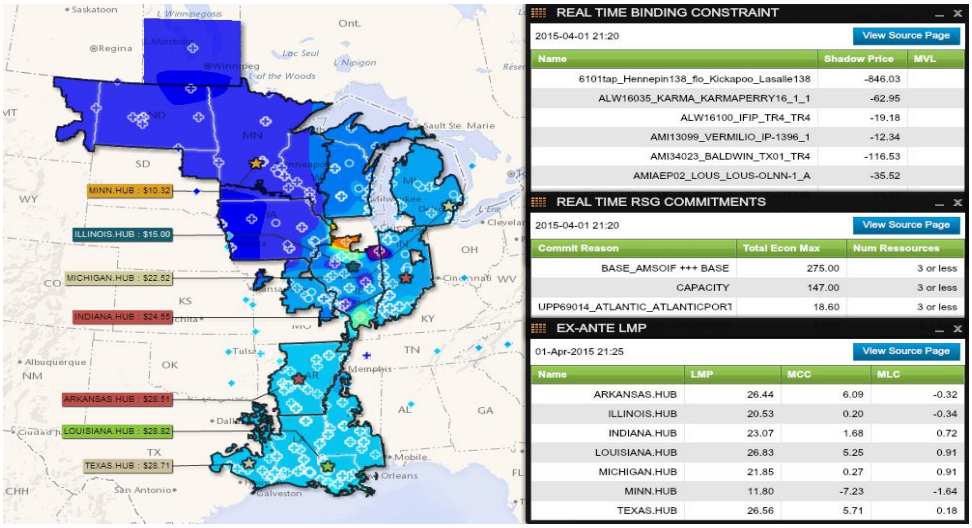

Figure 4. MISO LMP contour map (MISO, 2015)

In this thesis, the Unscented Transformation (UT) is used to solve POPF in a wind power integrated system. The UT method is used to accurately estimate the probability distribution of a nonlinearly transformed normal random variable based on a finite number of samples. The small data sample required in this method is an important attribute in large power systems. In this study, different scenarios are simulated in the IEEE standard test systems. Wind power is distributed as loads with negative power injection. The correlation between the loads and generators is also taken into account. The results from the study are compared with MCS.

CHAPTER 3

UNSCENTED TRANSFORMATION AND ITS APPLICATION TO PROBABILISTIC OPF

3.1. Introduction

One of the existing methods to estimate the statistical properties of a nonlinear system in response to random input variables is the Unscented Transformation (UT). The mean and covariance of the random variables are nonlinearly transformed to obtain the statistical properties of the output.

In the UT method, a set of weighted sigma points are selected so that certain properties of the input variables' PDFs are represented by the sample points. The nonlinear transformation is applied to all the sigma points and the statistical properties of the output variables are calculated using the sigma points and their respective weights, as shown Figure 5. Compared to other methods, the sigma points are selected in the UT to provide more information on the input PDFs, and the corresponding weights are not bounded between 0 and 1 as in other methods.

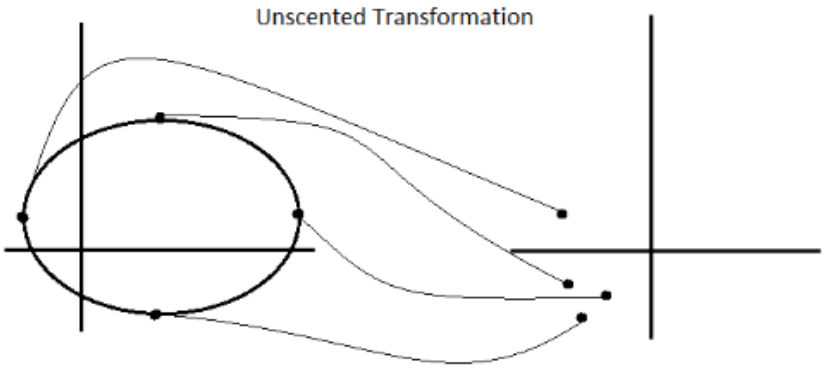

Figure 5. UT system model

In this Chapter, four UT methods are reviewed and two of them are formulated for POPF application and the results are compared to MCS.

3.2. Unscented Transformation

UT is based on a set of sample points known as sigma points that exhibit specific properties of PDFs. The sigma points and their corresponding weights are used to estimate the statistical properties of the output mean and covariance, with a limited number of computations. Selection of sigma points is a fundamental step to the success of the method. Four different UT methods are discussed in this section. Although UT is simple, it effectively solves nonlinear problems with less computation. The accuracy is the same as linearization to the second order.

A set of sigma points whose sample PDF approximates the true PDF are selected as the inputs of the nonlinear function to determine the corresponding output. The approximate mean and covariance of the output are determined with the weights using the following equations [25-27].

$$y^{(i)} = h\left(x^{(i)}\right) \tag{3.1}$$

$$\bar{y} = \sum_{i=0}^{n} W^{(i)} y^{(i)} \tag{3.2}$$

$$P = \sum_{i=0}^{n} W^{(i)} (y^{(i)} - \bar{y})(y^{(i)} - y)^{T} \tag{3.3}$$

where, x and y are the input and output vectors of the nonlinear function h and n is the number of sigma points for each variable. W is the weight vector that satisfies the condition:

$$\sum_{i=0}^{n} W^{(i)} = 1, \qquad i = 1,2, \dots, n \tag{3.4}$$

The results of the UT method match the true mean of the output up to third order [28-30]. In this thesis, a UT-based POPF algorithm is used to estimate the mean and covariance of the output.

3.3. UT Methods

3.3.1. Basic UT

In Basic UT, two points are selected to represent the distribution of each variable. The two points are such that one is greater and the other is lower than the mean value, with equal absolute difference from the mean value. 2n sigma points are formed using the following equations:

$$x^{(i)} = \bar{x} + \tilde{P}^{(i)} \quad i = 1, \dots, 2n \tag{3.5}$$

$$\tilde{P}^{(i)} = (\sqrt{nP})_{(i)}^{T} \quad i = 1, \dots, n \tag{3.6}$$

$$\tilde{P}^{(n+i)} = -(\sqrt{nP})_{(i)}^{T} \quad i = 1, \dots, n \tag{3.7}$$

where $\tilde{P}^{(i)}$ is the ith row of the matrix $\sqrt{nP}$. To get $\tilde{P}^{(i)}$, P must be positive definite. In power system, the factorization process is reduced since the covariance matrix is sparse. The weights for Basic UT are the same for all n variables.

$$W^{(i)} = \frac{1}{2n}, i = 1, \dots, 2n. \tag{3.8}$$

3.3.2. General UT

In this method, nonlinear transformation is achieved using $2n + 1$ sigma points. Compared to Basic UT method, one addition point that represents the mean is required as follows:

$$x^{(0)} = \bar{x} \tag{3.9}$$

$$x^{(i)} = \bar{x} + \tilde{P}^{(i)} \quad i = 1, \dots, 2n \tag{3.10}$$

$$\tilde{P}^{(i)} = (\sqrt{(n + k)P})^{T} \quad i = 1, \dots, n \tag{3.11}$$

$$\tilde{P}^{(n+i)} = -\left(\sqrt{(n + k)P}\right)^{T} \quad i = 1, \dots, n \tag{3.12}$$

The 2n+1 weighting coefficient are

$$W^{(0)} = \frac{K}{n+K} \tag{3.13}$$

$$W^{(i)} = \frac{K}{2(n+K)} \quad i = 1, \dots, 2n \tag{3.14}$$

Any K value can be used as long as $(n + K) \neq 0$. K can be used to reduce the high-order errors of the mean and covariance approximation. Basic UT is a special case of General UT.

3.3.3. Simplex UT

When the computational cost is a paramount, then few sigma points can be selected, since cost is proportional to the number of sigma points. The order of estimation can be reduced to n+1 points, which is the minimum number of points comprising the fixed mean and covariance value.

Selection of the weight $W^{(0)} \in [0,1)$, will only affect the fourth and higher order moments of the set of sigma points. The rest weights are as follows:

$$W^{(i)} = \begin{cases} 2^{-n}\left(1 - W^{(0)}\right) & i = 1,2 \\ 2^{i-2}W^{(1)} & i = 3, \dots, n+1 \end{cases} \tag{3.15}$$

Initialize the α vector

$$\alpha_0^{(1)} = 0 \tag{3.16}$$

$$\alpha_1^{(1)} = \frac{-1}{\sqrt{2W^{(1)}}} \tag{3.17}$$

$$\alpha_1^{(1)} = \frac{1}{\sqrt{2W^{(1)}}} \tag{3.18}$$

Recursively expand the σ vectors by performing the following steps for $j = 2, \dots n$

$$\alpha_j^{(i)} = \begin{cases} \begin{bmatrix} \alpha_0^{(j-1)} \\ 0 \end{bmatrix}, & i = 0 \\ \begin{bmatrix} \alpha_i^{(j-1)} \\ \frac{-1}{\sqrt{2W^{(j+1)}}} \end{bmatrix}, & i = 1, \dots, j \\ \begin{bmatrix} 0_{j-1} \\ j \\ \frac{}{\sqrt{2W^{(j+1)}}} \end{bmatrix}, & i = j+1. \end{cases} \tag{3.19}$$

0_j is the column vector containing j zeros.

After the n-element vectors $\alpha_i^{(n)} (i = 0, \dots, n+1)$. The sigma points are as follows:

$$x^{(i)} = \bar{x} + \sqrt{P}\alpha_i^{(n)} \qquad (i = 0, \dots, n+1) \tag{3.20}$$

In this method, n+1 sigma points are used since $W^{(0)} = 0$. The weights for simplex UT increase geometrically. For a system of high-dimension, this method can cause

problems, such as overflow and quantization of errors. Therefore, the method saves computational time, but is not suitable for high-dimension nonlinear systems.

3.3.4. Spherical UT

The spherical UT uses n+2 spherical sigma points. The algorithm is the same for finding the sigma points, except that

$$W^{(i)} = \frac{1-W^{(0)}}{n+1}, \quad i = 1, \dots, n+1 \tag{3.21}$$

$$\alpha_j^{(j)} = \begin{cases} \begin{bmatrix} \alpha_{j-1}^{(0)} \\ 0 \end{bmatrix}, & i = 0 \\ \begin{bmatrix} \alpha_{j-1}^{(i)} \\ -1 \\ \hline \sqrt{j(j+1)W^{(1)}} \end{bmatrix}, & i = 1, \dots, j \\ \begin{bmatrix} 0_{j-1} \\ 1 \\ \hline \sqrt{j(j+1)W^{(1)}} \end{bmatrix}, & i = j+1. \end{cases} \tag{3.22}$$

Compared with simplex UT, spherical UT uses equal weights and is less computationally intensive.

3.4. Unscented Transformation for Probabilistic Optimal Power Flow

The standard model for the POPF is [28]:

$$Y = g(X)$$

$$Z = h(X)$$

where, X is the input vector, such as voltage magnitudes and angles. Y is the state random vector from normal distribution function [31], Z is output vector. g is the power injection function, and h is the OPF function. Z and Y can vary depending on the problem being evaluated. The mean and covariance of all the loads including P_{wind} and P_{load} are known. As shown in the following equations:

$$Z = \begin{bmatrix} \delta \\ V \\ P_G \\ Q_G \\ P_{loss} \\ LMP \\ \dots \end{bmatrix} \tag{3.23}$$

$$Y = \begin{bmatrix} P_{wind} \\ P_{load} \end{bmatrix} \tag{3.24}$$

where δ is the voltage angle, V is voltage magnitude, P_G and Q_G are the real and reactive power of the generators. P_{loss} is the system real power loss and LMP is the locational marginal price. P_{wind} is the real power generated by the wind and P_{load} is the real power of the load demand.

In this study, the simulation results are determined by LMPs which are mostly used in the power market by ISOs to operate the system and manage power balance. LMP are solved by running OPF, which facilitates the management of the power market and determines electricity pricing to the different Utilities ahead of time or in real-time.

Sigma points are obtained from the normal distribution function:

$$P(x) = \frac{1}{\sigma\sqrt{2\pi}} e^{(x-\mu)^2/(2\sigma^2)} \tag{3.25}$$

where, μ and σ are the mean and variance.

In an OPF problem, constraints are added to the objective function by using Lagrange multipliers. The optimization process yields optimal solutions for state variables in order to minimize the total cost while ensuring the system stability and security. Unlike OPF, input variables in POPF are represented by the sigma points from probability distribution functions, determined by the UT method, instead of using constant values. The POPF calculation steps are as follows:

$Step$ 1: Set the input vector, including the mean vector x and covariance matrix P for all the loads power demand

$$\mathrm{X} = \begin{bmatrix} P_{wind} \\ P_{load} \end{bmatrix}$$

$Step\ 2$: Determine the sigma points for all the loads and wind power using the UT methods. In this study, Basic and General UT methods are used to obtain the sigma points, in which 2n and 2n+1 sigma points are required respectively.

$Step\ 3$: Set the power of the loads using the sigma points obtained, and run OPF function using MATLAB. Data of the system is acquired from MATPOWER files.

$Step\ 4$: Use equations (3.1)-(3.3) to analyze the distribution of output LMP based on the output data.

Note that the covariance matrix P for loads and wind power are obtained from the correlation matrix. The relationship is as follows

$$\mathrm{S} = \mathrm{D} * \mathrm{R} * \mathrm{D} \tag{3.26}$$

where S is the covariance matrix, D is the diagonal matrix from standard deviation of all loads, and R is the correlation matrix that varies with the system network.

To verify the effectiveness of the method in estimating the statistical properties of the LMPs, results are compared with the simulation results from MCS. The relative errors of the calculated mean (μ) and standard deviation (σ) are calculated as

$$\varepsilon_{\mu} = \frac{|\mu_{MCS} - \mu_{UT}|}{\mu_{MCS}} \times 100\% \tag{3.27}$$

$$\varepsilon_{\sigma} = \frac{|\sigma_{MCS} - \sigma_{UT}|}{\sigma_{MCS}} \times 100\% \tag{3.28}$$

where, ε_{μ} and ε_{σ} are the mean and standard deviation of the errors, μ_{MCS} and σ_{MCS} are the mean and standard deviation values of LMPs from MCS, μ_{UT} and σ_{UT} are the mean and standard deviation values from UT-based POPF.

The average error between the MCS and the UT method is also defined as

$$\varepsilon_{\mu}^{AVG} = \frac{1}{N_{bus}} \sum_{i=1}^{N_{bus}} \varepsilon_{\mu}(i) \tag{3.29}$$

$$\varepsilon_{\sigma}^{AVG} = \frac{1}{N_{bus}} \sum_{i=1}^{N_{bus}} \varepsilon_{\sigma}(i) \tag{3.30}$$

where ε_{μ}^{AVG} is the average error of the mean. $\varepsilon_{\sigma}^{AVG}$ is the average error of the STD. $\varepsilon_{\mu}(i)$ is the error in mean between MCS and UT at bus i. $\varepsilon_{\sigma}(i)$ is the error in STD between MCS and UT at bus i and N_{bus} is the number of bus.

The Basic and General UT-based POPF algorithm is evaluated through simulation results of the standard IEEE test cases. Different case studies are simulated to assess the performance of the proposed POPF with respect to wind power generation, location, and load correlations. The mean and variance of the UT-based POPF algorithm output (i.e. LMPs) are calculated and compared with MCS method. The simulation results and discussions are presented in the following chapter.

CHAPTER 4

SIMULATION RESULTS AND DISCUSSION

4.1. Introduction

In this Chapter, POPF algorithm based on Basic and General UT method are evaluated on the IEEE 30- and 118-bus power transmission systems. Different case studies, including wind farm locations, wind power penetration levels are assessed to evaluate the performance of the proposed method. The LMP results simulated from MCS method are used as validation for the UT-based results.

4.2. The IEEE Standard Test Systems

In this study, the loads are assumed to be random variables with normal PDF of known mean and variance. Load patterns are assumed to be the same within specified geographical areas, depending on the weather, seasons and other factors, such as peak hours of electricity demand. Integrated wind power is simulated as a negative load with a normal PDF. Several wind farms are located in the power grid, where they are modeled as independent or correlated random variables. The load demands and wind power integration are assumed to be mutually independent. In order to test the effectiveness of the UT-based POPF algorithm, different case scenarios are simulated on the IEEE 30- and 118-bus system in MATPOWER [32]. These IEEE test cases represent a portion of the American Electric Power (AEP) transmission system in the Midwestern US.

4.2.1. The IEEE 30-bus System

The IEEE 30-bus system consists of 6 generators, 20 loads and 41 branches as shown in Figure 6 [33]. The total generator capacity is 335 MW and the total load is 189.2 MW. The loads are modeled as a normal PDF with known means and variances (e.g. variance is 5% of the mean). The mean values of the loads are provided in Table 1.

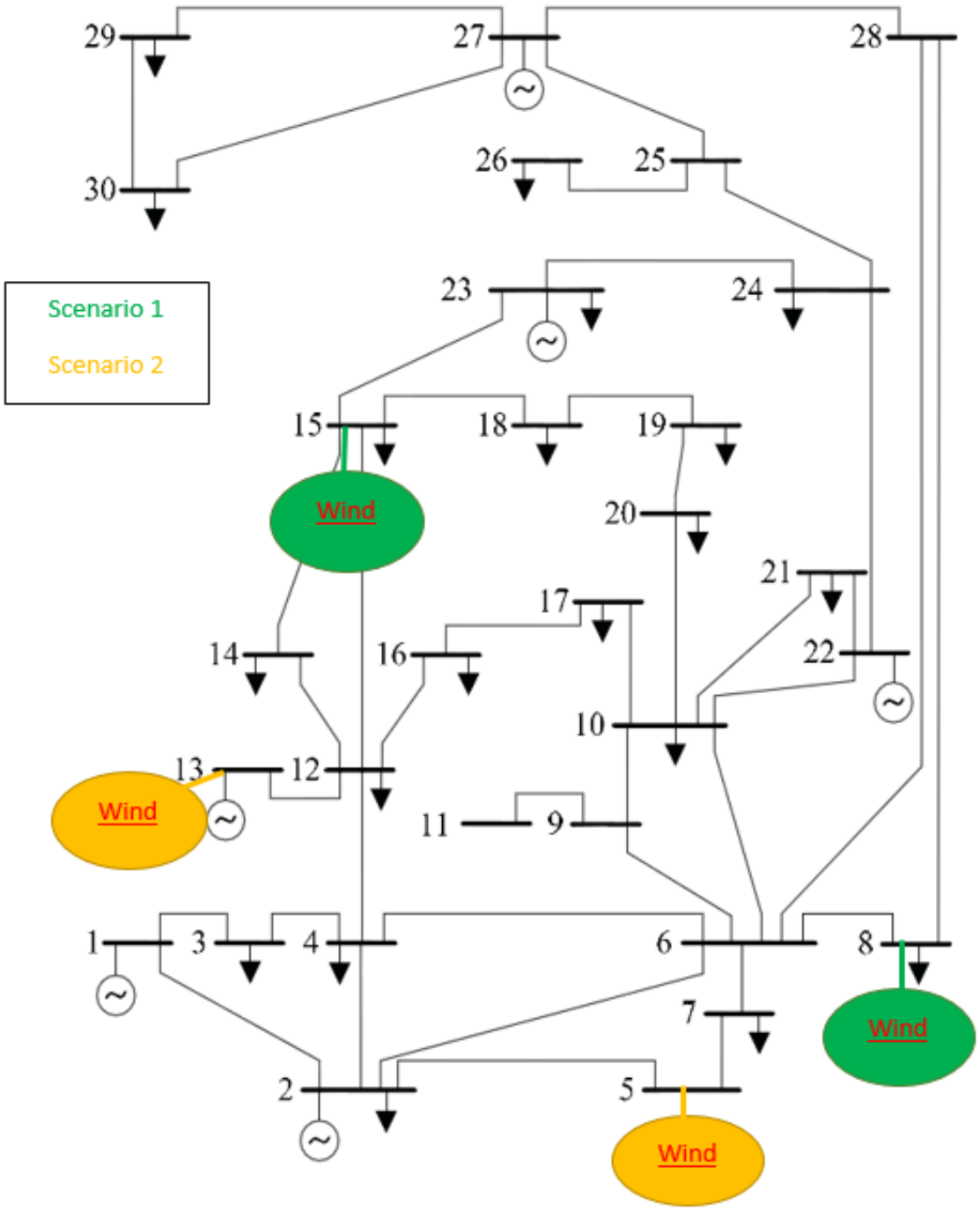

Figure 6. Signal line diagram of the IEEE 30-bus test system

Table 1. Bus loads in the IEEE 30-bus system

Bus	Load(MW)	Bus	Load(MW)
1	0.0	16	3.5
2	21.7	17	9.0
3	2.4	18	3.2
4	67.6	19	9.5
5	34.2	20	2.2
6	0.0	21	17.5
7	22.8	22	0.0
8	30.0	23	3.2
9	0.0	24	8.7
10	5.8	25	0.0
11	0.0	26	3.5
12	11.2	27	0.0
13	0.0	28	0.0
14	6.2	29	2.4
15	8.2	30	10.6

All the loads and wind power are represented by normal PDFs. Wind power generation is considered as a negative power input in forms of Gaussian PDF with known mean and variance.

Different case studies are carried out to evaluate the UT-based POPF with respect to wind farm location and wind power generation capacities. Both independent and correlated random variables (i.e., loads and wind generation) are studied. For the independent random variables, the mean and variance of each individual load and wind power capacities are selected accordingly. For the correlated random loads, we partitioned the IEEE 30-bus system into small parts to take into account the correlation between the loads within the same geographical locations, as shown in Figure 7.

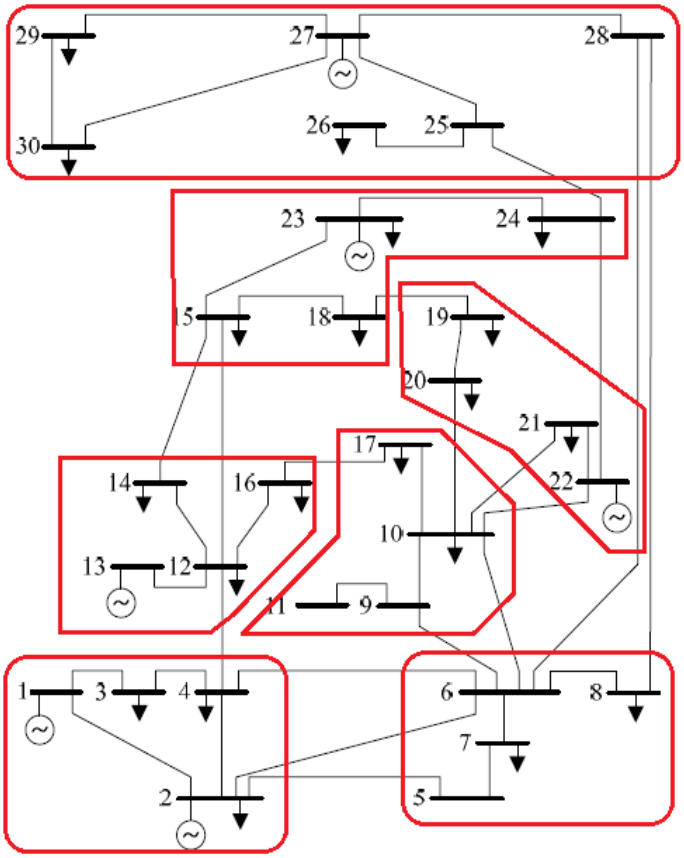

Figure 7. The IEEE 30-bus system with correlated small parts

All the buses within the small partitions are mutually correlated and represented by a correlation matrix. Thus, several correlation matrices corresponding to each geographical location of the grid form the correlation matrices of the entire transmission system. The covariance matrix for each small location is calculated using equation (3.26). Working with a stacked covariance matrix developed for the entire system has two benefits: (i) increase in accuracy of the covariance matrix formation, and (ii) reduction in the computing burden. Note that each covariance matrix is a positive definite symmetric matrix and represents the covariance between the correlated loads.

4.2.2. The IEEE 118-bus System

The IEEE 118-bus system includes 19 generators, 9 transformers, 99 loads and 186 transmission lines, as shown in Figure 8 [33]. Bus 69 is the reference bus (i.e. voltage

magnitude is 1 pu and voltage angle is 0) and the voltage angles at all other buses are calculated with respect to the reference bus. The total load demand of the system is 4519 MW, and the total generator capacity is 5859 MW, of which the actual power generated is 4319.4 MW at one snap-shot.

Different case studies are used to evaluate the proposed POPF in different conditions. In all scenarios, the loads and wind power are mutually independent. However in case studies with correlated loads, a correlation matrix is used to show the relationship between the neighboring loads. The IEEE 118-bus system is also divided into small parts to simplify the calculation of the correlation matrices associated with each neighboring area. In each small parts, nearby buses are correlated with each other and their relationship is represented by equation (3.26).

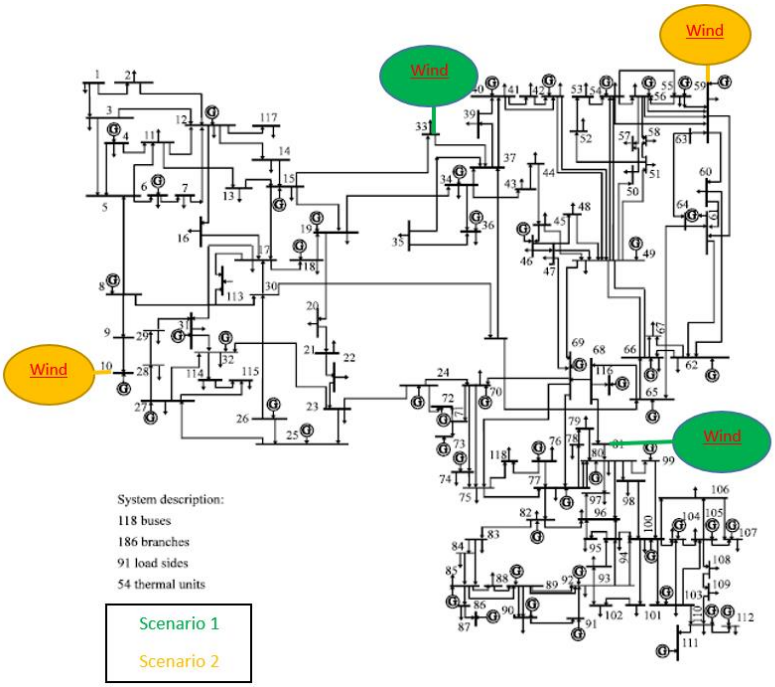

Figure 8. Signal line diagram of the IEEE 118-bus test system

4.3. Case Studies

For all case studies, the results are obtained by running the POPF in MATLAB. The results of the Basic and General UT-based POPF are compared with simulation results from MCS methods to assess the performance of the proposed algorithm.

Case 1: Load Uncertainty

On the IEEE 30-bus system, two wind farms are located at bus 8 and 15, as shown in the green circles in Figure 6, in order to disperse the wind power generation [34-35]. The capacities of the wind farms are 200 and 150 MW, respectively. At a given snap-shot, the means for the wind power are 15% and 30% of their power capacities and the variances are 15% and 17% of their mean values.

On the IEEE 118-bus system, two wind farms are located at bus 33 and 81, shown in green circles in Figure 8. The capacity of the two wind farms are 2500 and 3500 MW. At the studied snap-shot, the means for the wind generations are 636.3 and 1272.6 MW, respectively. The variances are 15% and 17% of the mean values, respectively. Case 1 is used as the reference for other case studies, when the distribution of the loads is changed. In both test cases, uncorrelated loads are modeled as mutually Gaussian PDFs with known mean and the variance that are 5% of the mean values.

Case 2: Wind Farm Location

To assess the effect of wind farm locations on the proposed POPF performance, wind farm locations are changed. With more wind power integrated into the system to supply the loads, price of electricity can be reduced. However, the uncertainties in wind power complicate the forecasting of the system states. Loads that are located near to the wind farms can be impacted by the fluctuation of wind power. Different locations of the wind farms have significant influences to the POPF output. In the IEEE-30 bus system, wind

farms are assumed to be located at bus 5 and 13 shown in yellow circles of Figure 6. These are located at the periphery of the system in order to reduce the forecasting errors. In the IEEE-118 bus system, wind farms are connected to bus 10 and 59, as shown in the yellow circles of Figure 8. The calculated statistical properties of the LMPs are provided to assess the performance of the method.

Case 3. Wind Power Generation

Wind power generation is varied to evaluate the performance of the proposed algorithm with respect to the wind power generation levels. Low variance of LMPs is expected when the amount of wind power is reduced.

In the IEEE-30 bus system, two wind farms are connected to bus 8 and 15, similar to case 1. The total load is reduced to 260 MW. The wind farm with 150 MW capacity generates power with the mean = 22.5 MW and variance = 3.375 MW. The other wind farm with 200 MW capacity generates power with the mean = 16 MW and variance = 2.72 MW. On the IEEE 118-bus system, one of the wind farms stays constant and the other one is varied to have the power mean and variance of 339.36 MW and 57.6912 MW respectively.

4.4. Results and Discussions

The Basic UT and General UT methods are used for the case studies. Both independent and correlated loads are included in the studies. Different bus systems are used to simulate the system, in which the loads were assumed to be normally distributed with known mean and variance. Wind power is also assumed to be normally distributed and treated as a negative load. For the independent load conditions, there is no correlation between the loads, and the wind farms are also mutually independent. For

system with correlated loads, correlation matrices are formed between nearby loads depending on their locations in the network.

MCS is used to evaluate the accuracy and performance of the UT-based POPF algorithm. Similar network configurations and parameters were used to operate the power flow process for both UT-based POPF and MCS. Results from the UT-based methods are compared to the results from MCS using equations (3.27-3.28). Performance of the methods are assessed and tested on the IEEE 30- and 118-bus system.

4.4.1. Independent Loads

- **The IEEE-30 bus system**

Results from the IEEE 30-bus study using the Basic and General UT method with independent loads are shown in Figures 9 and 10. The average of the mean and standard deviation errors calculated using (3.29) and (3.30) for all three case studies are presented in Table 2. Figure 9 shows the mean error of the Basic UT method on the IEEE 30-bus system compared with the results from MCS methods. Mean errors are relatively small in Cases 1 and 3 with most points are within 2% error. Thus, the measurement errors are acceptable. The results of Case 3 show that wind farm locations can influence the system performance and that the closer locations to the wind farm lead to larger errors.

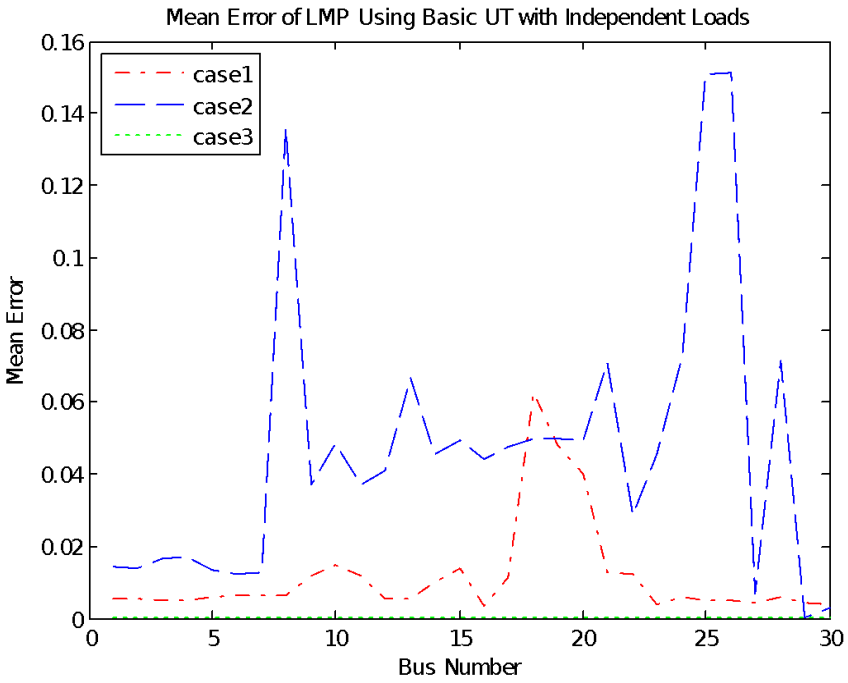

Figure 9. Mean error of basic UT with independent loads on the IEEE 30-bus system

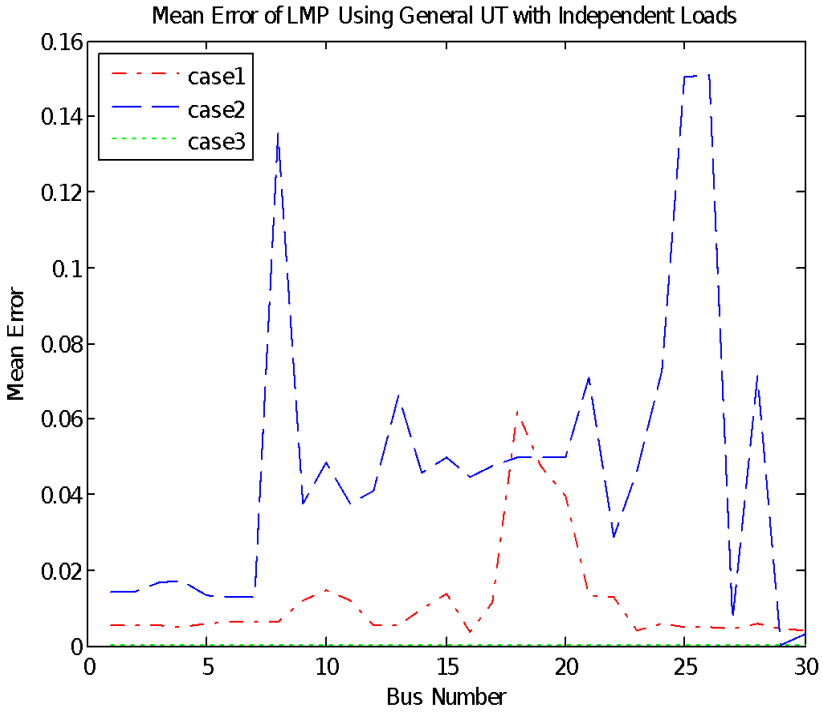

Figure 10. Mean error of general UT with independent loads on the IEEE 30-bus system

Table 2. Average mean error with independent loads on the IEEE 30-bus system

Method	Case 1		Case 2		Case 3	
	Mean	STD	Mean	STD	Mean	STD
Basic UT	0.0116	0.4184	0.0468	0.7451	0.0002	0.2281
General UT	0.0116	0.4068	0.0469	0.7415	2.4e-05	0.1990

Figure 10 shows the results of the General UT-based POPF on the IEEE 30-bus system. As shown in Figure10, the mean errors from the General UT method are comparable to the MCS method. Similar to the results of the Basic UT method, both Case 1 and Case 3 have smaller errors within 2% error range, whereas, errors from Case 2 are bigger due to the changes of the wind farm locations. There are also slightly larger errors in the buses that are directly connected to the wind farms in all the cases. For example, the trend for the General UT method in Figure 10 shows that the errors are larger for the buses closer to the wind farms (i.e., bus 8 and 15).

- **The IEEE 118-bus System**

Errors between the calculated mean using the UT-based and the MCS are shown in Figures11 and 12. The results in Figure 11 show that most of the mean errors for LMP in the Basic UT-based POPF are within 5% of MCS results. With a lower level of wind power penetration in Case 3, the mean errors become smaller. However, locations of the wind farms have more impact on the LMPs as shown in Figure 11, Case 2.

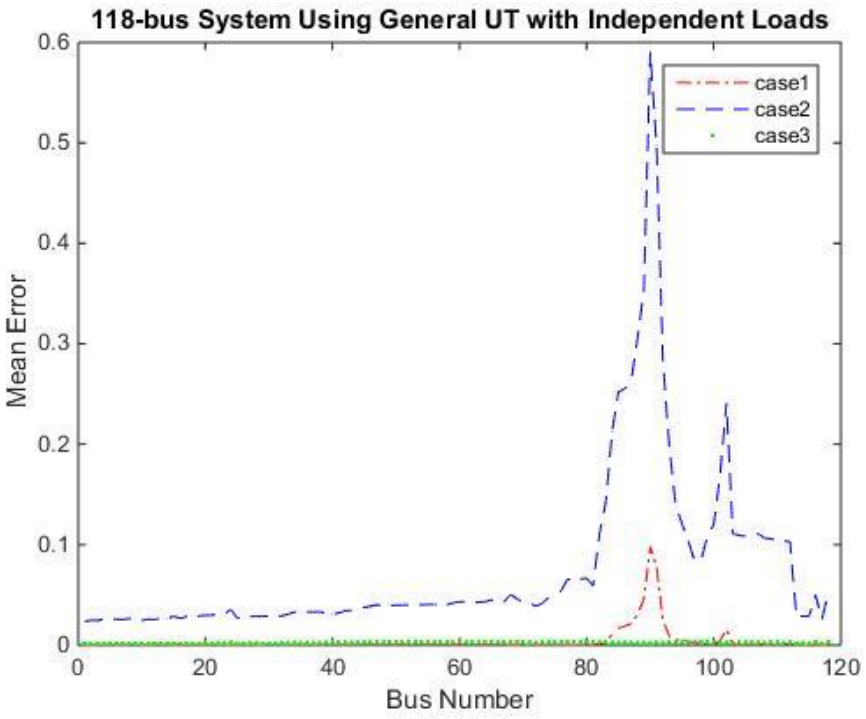

Figure 11. Mean error of the basic UT with correlated loads on the IEEE 118-bus system

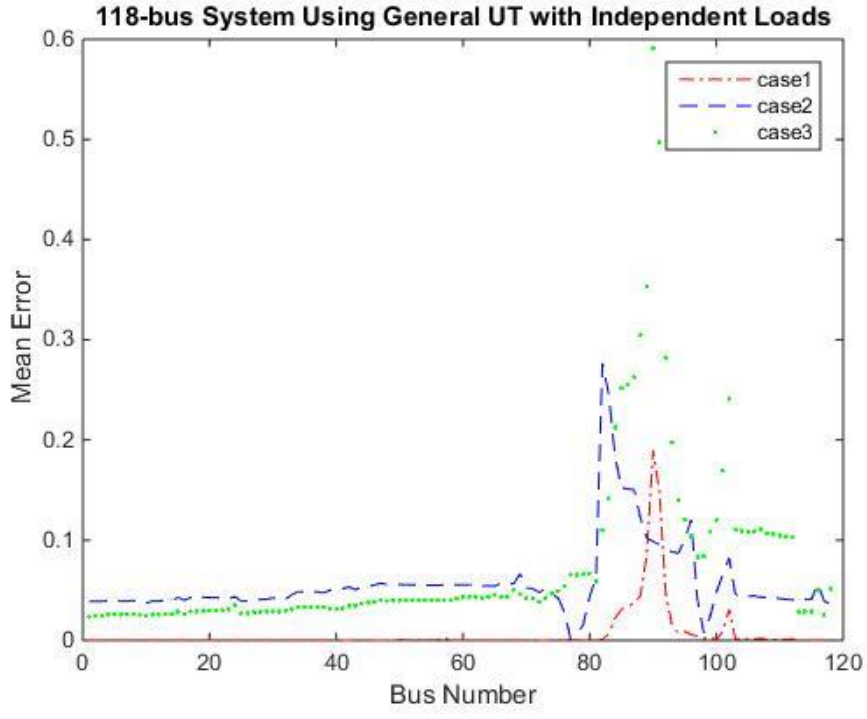

Figure 12. Mean error of the general UT with independent loads on the IEEE 118-bus system

Figure 12 shows the mean errors of LMPs obtained from the General UT relative to MCS results. For most of the buses in Case 1 and Case 3, the mean errors of LMPs are smaller and within 5% range of MCS, which demonstrates the effectiveness of the General UT method. Similar to the IEEE 30-bus system, wind farm locations change the LMPs and introduced larger mean errors in Case 2. The results for both Basic and General UT indicate that mean errors of LMPs for buses located closer to the wind farms are larger than other buses.

4.4.2. Correlated Loads

- **The IEEE 30-bus System**

Neighboring loads are typically mutually correlated since they are affected by the same factors, such as the weather. Resolving all the correlated variables adds to the computing burden. To solve this problem, the IEEE 30 bus system is divided into small parts as shown in Figure 1. This is justifiable since closely connected buses have stronger correlation patterns, and the covariance of loads that are far apart are negligible. With each small part analyzed separately, the problem is simplified and the computing burden is reduced. It is also assumed that there is no correlation between the wind power and the loads.

A positive definite correlation matrix is formed based on the configuration of the IEEE test system. On the IEEE 30-bus system, the correlation matrix of the small parts consisting of buses 1, 2, 3 and 4 is

$$R = \begin{bmatrix} 1 & 0.38 & 0.47 & 0.41 \\ 0.38 & 1 & 0.45 & 0.47 \\ 0.47 & 0.45 & 1 & 0.55 \\ 0.41 & 0.47 & 0.55 & 1 \end{bmatrix}$$

This covariance matrix shows the relationship between all the variables obtained from equation (3.26). Results of the Basic and General UT with correlated load are provided in Figures 13 and 14.

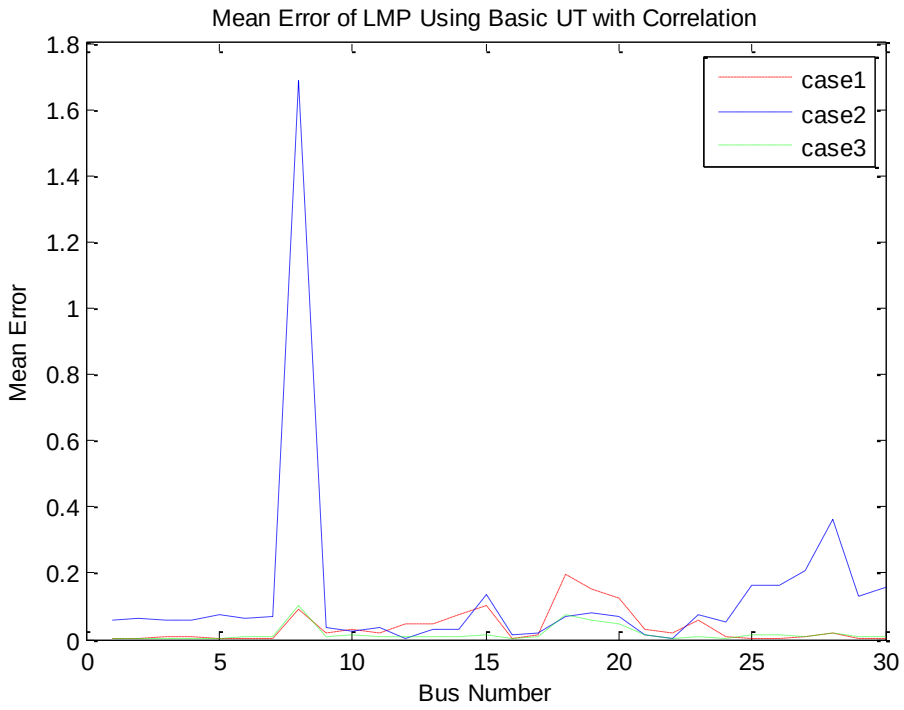

Figure 13. Mean error of basic UT with correlated loads on the IEEE 30-bus system

As observed in Figure 13, the relative errors in Case 1 and 3 are around 8%, which is within the acceptable range. In Case 2, the errors are bigger due to the changes in locations of the wind farms. By comparing the independent and correlated loads in Figure 10 and 14, it is observed that the Basic UT-based method lead to bigger relative errors with correlated loads compared to independent loads.

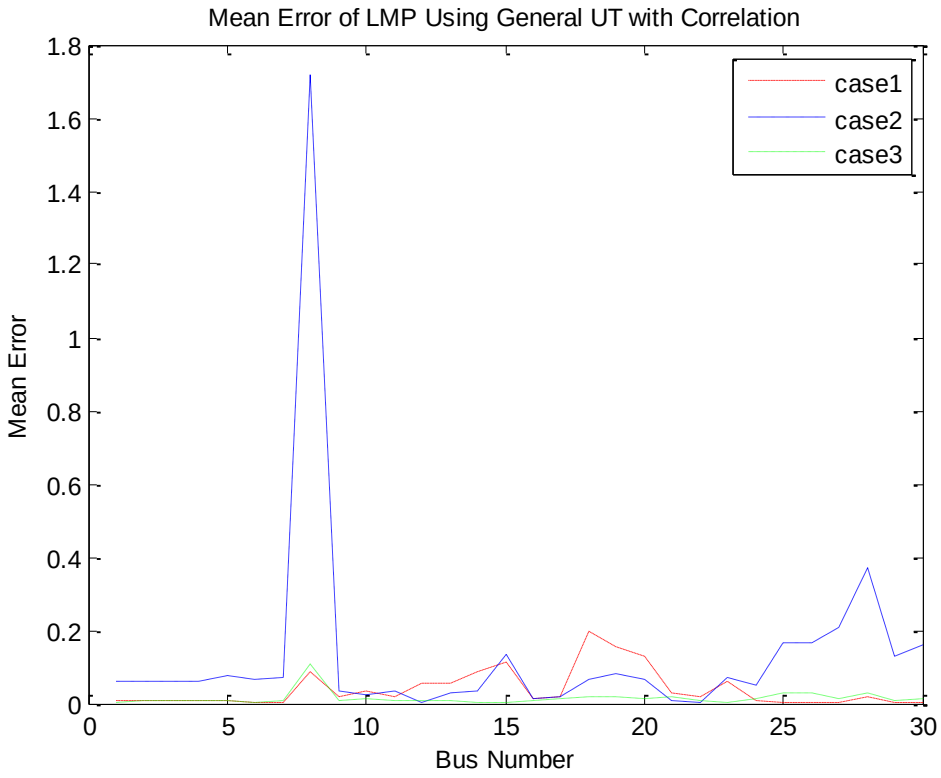

Figure 14. Mean error of general UT with correlated loads on the IEEE 30-bus system

However, as it is observed in Figure 14, the relative errors of the General UT-based POPF are smaller on the IEEE 30-bus system with correlated loads compared to the one with independent loads. Furthermore, in both Basic and General UT methods, the errors are less than 10%, especially in Cases 1 and 3. With less wind power penetration, the mean errors decreased to less than 5%, which demonstrates the influence of wind farm locations on the LMPs. Increased wind power penetration and the closeness of the wind farm locations have significant influence on market variability as captured by LMPs.

- **The IEEE 118-bus System**

The IEEE 118-bus system is also divided into small parts to show the correlation between the nearby loads. The relative errors of the estimated LMP mean at all the buses are shown in Figures 15 and 16. Most of the buses have relative errors less than

5% in all three cases, and are greater for the buses located closer to the wind farms. By comparing the three cases, it is observed that Case 2 has larger relative errors, further demonstrating that the locations of wind farms have significant influence on the accuracy of the LMP estimation. In Case 3, when wind power generation is decreased, the reduction in wind power fluctuations lead to less uncertainty in LMP estimation.

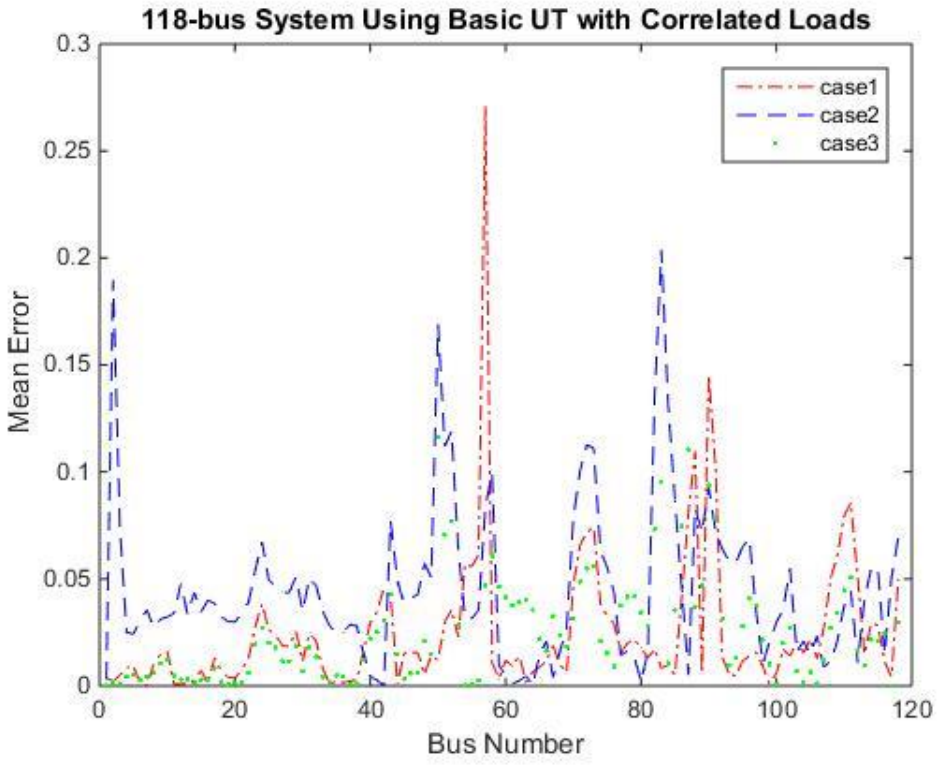

Figure 15. Mean error of the basic UT with correlated loads on the IEEE 118-bus system

The average of the mean and standard deviation errors calculated using (3.29) and (3.30) for all three case studies are presented in Table 3. The UT-based POPF method is capable of estimating the statistical properties of LMP (i.e., mean and variance) with an acceptable error range for practical power system operations.

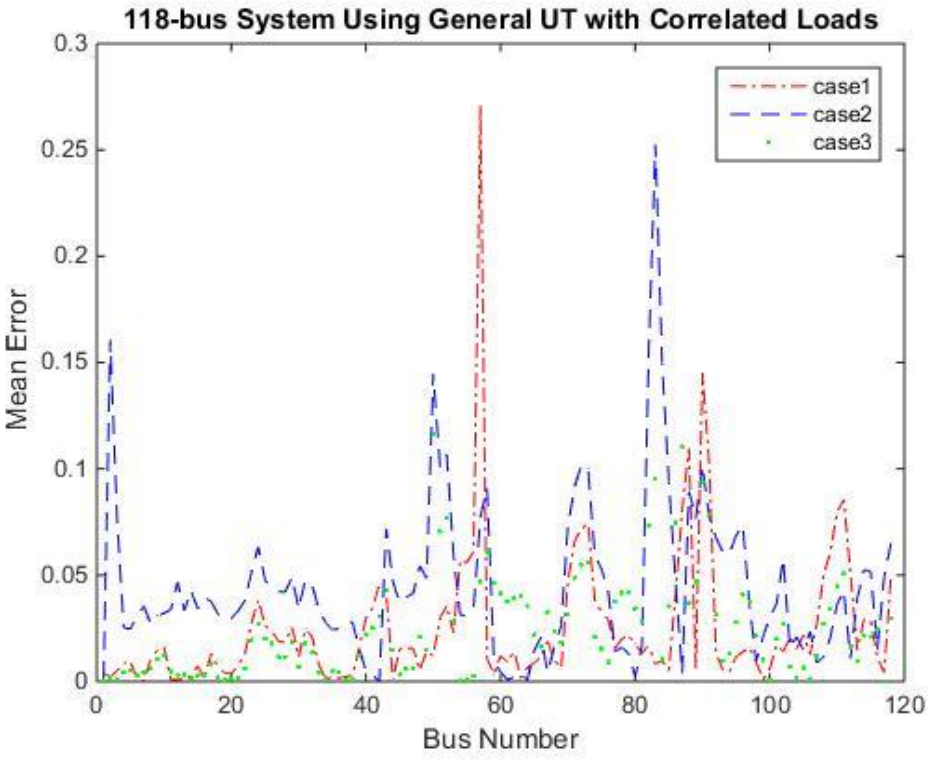

Figure 16. Mean error of the general UT with correlated loads on the IEEE 118-bus system

Table 3. Average mean errors with correlated loads on the IEEE 118-bus system

Method	Case 1		Case 2		Case 3	
	Mean	STD	Mean	STD	Mean	STD
Basic UT	0.0369	0.2810	0.1342	0.4564	0.0168	0.9874
General UT	0.0394	0.2757	0.1348	0.4304	0.0143	0.2659

CHAPTER 5

CONCLUSION AND FUTURE WORK

The increasing proliferation of large-scaled renewable energy-based power generation has added more challenges to secure power system operation. The stochastic nature of renewable-based energy sources adds more uncertainty to the output of power system operation tools, such as optimal power flow (OPF). Therefore, probabilistic optimal power flow (POPF) was introduced in power systems community to deal with the stochastic variables (e.g., renewable resources and uncertain loads). In this study, a new POPF algorithm is proposed that is based on the Unscented Transformation (UT). Basic and General UT methods are evaluated for POPF and are then compared to Monte Carlo Simulation (MCS). The input random variables are assumed to have a normal probability distribution function (PDF). The UT-based algorithm uses fewer sampling points to represent the PDFs and since no linearization process is involved in its formulation, it reduces the computation load. In this study, the accuracy of the UT-based POPF algorithm was evaluated using locational marginal price (LMP) in the power transmission network. LMP is the price of electricity in high-voltage transmission market, which is calculated by a non-profit organization for power system and market operation referred to as the independent system operator (ISO). ISOs are responsible for clearing the day-ahead and real-time market for all market participants including power generators, load serving entities (LSE), transmission owners (TO) etc.

Different test cases of the IEEE 30- and 118-bus transmission systems were simulated to assess the uncertainties from input random variables (e.g., wind power output, load), wind farm locations and different levels of wind power penetration. It was observed that the proposed algorithm matched the simulation from MCS, which were regarded as the benchmark. For the next step, the performance of the algorithm was evaluated

for several wind farms locations. The wind farm locations significantly influenced the results as depicted by the mean errors of the LMP. It was observed that the estimated mean and variance of the LMPs at the buses that were located near the wind farms, had more errors relative to MCS. In addition, the extensive case studies proved that the LMP mean and variance errors were smaller in systems with correlated loads than in the systems with independent loads.

While UT-based POPF is demonstrated and simulated in this thesis, future research is required to utilize all four type of UTs for POPF in large transmission grids (e.g., The IEEE 300-bus and NV Energy 340-bus systems) to evaluate the efficiency and accuracy of the proposed algorithm, and select the UT with the optimal performance. Moreover, other POPF output (e.g., total generation cost, total lost) should also be considered to evaluate the UT-based POPF algorithm. Future work is also necessary to identify the best locations for the renewable energy generation to minimize the total generation cost.

REFERENCE

[1] H. Saadat, *Power System Analysis*. Third Edition. PSA Publishing, 2010.

[2] Power System Network, from http://energy.gov/science-innovation

[3] K. Ali, N. M. Mogammad and D. Min, *Integration of Green and Renewable Energy in Electric Power Systems*. Wiley, ISBN: 978-0-470-18776-0, Dec. 2009.

[4] A. Thomas, *Wind Power in Power System*. Second Edition. John &Sons, Ltd. 2012.

[5] Global Wind Energy Council, *Global Wind Report Annual Market Update 2011*. May. 2011.

[6] R. Wiser, M. Bolinger, *2012 Wind Technologies Market Report*. Berkeley (CA), U.S Department of Energy, Lawrence Berkeley Laboratory, 2013.

[7] Day Ahead Wind Forecast, from https://www.misoenergy.org/MarketsOperations

[8] B. Borkowska, "Probabilistic load flow," *IEEE Trans. Power Apparatus and Systems*, vol. PAS-93, no. 3, pp. 752-755, May-June. 1974.

[9] J. B. Ward and H. W. Hale, "Digital computer solution of power flow problems," AIEE Tansactions on Power Apparatus and Systems, vol. PAS-75, pp. 398-404, June. 1956

[10]. J. D. Glover, M. S. Sarma, and T. J. Overbye, *Power System Analysis and Design*. Fifth Edition. Publisher: Cengage Learning, Jan. 2011.

[11] D. Villanueva, J. L. Pazos and A. Feijoo, "Probabilistic load flow including wind power generation," *IEEE Transaction on Power Systems*, vol. 26, pp. 1659-1667, 2011.

[12] R. G. Brown and P. Y. C. Hwang, Introduction to Random Signals and Applied Kalman Filtering. Fourth Edition. John Wiley & Sons, Inc. New York, 2012.

[13] G. Verbic, A. Schellenberg, W. Rosehart, and C. A. Canizares, “Probabilistic optimal power flow applications to electricity markets,” International Conference on Probabilistic Methods Applied to Power Systems, pp. 1-6, June. 2006.

[14] P. Jorgensen, “Probabilistic load flow calculation using Monte Carlo techniques for distribution network with wind turbines,” *Harmonics and Quality of Power Proceedings 8th*, vol. 2, Oct. 1998.

[15] R. N. Allan, A. M. Leite da Silva, A. A. Abu-Nasser, and R. C. Burchett, “Discrete convolution in power system reliability,” *IEEE Trans. Rel*., vol. 30, no. 5, pp. 452–456, Dec. 1981.

[16] A. M. Leite da Silva, V. L. Arienti, “Probabilistic load flow by a multilinear simulation algorithm,” *IEEE Proc. on Generation, Transmission and Distribution*, vol. 137, issue 4, pp.276- 278, July. 1990.

[17] A. Schellenberg, W. Rosehart, and J. Aguado, “Cumulant based probabilistic optimal power flow (P-OPF)”, *International Conference on Probabilistic Methods Applied to Power Systems*, Ames, LA, USA, pp. 506-511, 2004.

[18] W. Tian, D. Sutanto, Y. Lee, and H. Outhred, “Cumulant based probabilistic power system simulation using Laguerre polynomials,” *IEEE Trans. Energy Convers*, vol. 4, no. 4, pp. 567–574, Dec. 1989.

[19] T. Williams and C. Crawford, “Probabilistic load flow modeling comparing maximum entropy and Gram-Charlier probability density function Reconstructions,” *IEEE Trans. Power System*, vol. 28, pp. 272-280, Dec. 2013.

[20] J. Usaola, “Probabilistic load flow with wind production uncertainty using cumulants and Cornish–Fisher expansion,” *16th PSCC*, Glasgow, Scotland, July. 2008.

[21] Y. Shu-jun and W. Yan, "Cornish-fisher expansion for probabilistic power flow of the distribution system with wind energy system," *Electric Utility Deregulation and Restructuring and Power Technologies (DRPT)*, pp. 1378-1383, 2011.

[22] H. P. Hong, "An efficient point estimate method for probabilistic analysis," *Reliab. Eng. Syst. Saf.*, vol. 59, pp. 261–267, 1998.

[23] J. M. Morales and J. Pérez-Ruiz, "Point estimate schemes to solve the probabilistic power flow," *IEEE Transactions on Power Systems*, vol. 22, no. 4, pp. 1594–1601, 2007.

[24] Location Marginal Pricing, from: http://www.iso-ne.com

[25] C. L. Su, "Probabilistic load-flow computation using point estimate method," *IEEE Trans. Power Systems*, vol. 20, no. 4, pp. 1843-1851, Nov. 2005.

[26] G. Verbic and C. A. Canizares, "Probabilistic optimal power flow in electricity markets based on a Two-Point estimate method," *IEEE Trans. Power System*, vol. 21, pp. 1883-1893, Nov. 2006.

[27] A. Monticelli, "Electric power system state estimation," *Proceedings of the IEEE*, vol. 88, no. 2, pp. 262-282, Feb. 2000.

[28] D. Simon, *Optimal State Estimation: Kalman, H Infinity, and Nonlinear Approaches.* John Wiley & Sons, Inc. New Jersey, 2006.

[29] S. Jafarzadeh, C. Lascu and M. S. Fadali, "State estimation of induction motor drives using the unscented kalman filter," *IEEE Trans. Industrial Electronics*, vol. 59, Nov. 2011.

[30] S. J. Julier and J. K. Uhlmann, "Unscented filtering and nonlinear estimation," *Proceedings of the IEEE*, vol. 92, Mar. 2004.

[31] O. A. Oke, D. W. P. Thomas, G. M Asher and L.R.A.X de Menexas, "Probabilistic load flow for distribution systems with wind production using Unscented

Transform method," *Innovative Smart Grid Technologies (ISGT)*, 2011 IEEE PES, Jan. 2011.

[32] R. D. Zimmerman, C. E. Murillo-Sánchez, and R. J. Thomas, "MATPOWER Steady-State operations, planning and analysis tools for power systems research and education," *Power Systems, IEEE Transactions*, vol. 26, no. 1, pp. 12-19, Feb. 2011.

[33] M. A. Abido, "Optimal power flow using particle swarm optimization," International Journal of Electrical Power Energy Systems, vol. 24, no. 7, pp. 563–571, 2002.

[34] R. N. Allan, B. Borkowska and C. H. Grigg, "Probabilistic analysis of power flows," *Proceedings of the Institution of Electrical Engineers*, vol. 121, no. 12, pp. 1551-1556. London, Dec. 1974.

[35] Y. Chang, T. Lee, C. Chen and R. Jan, "Optimal power flow of a wind-thermal generation system," *Electrical Power and Energy Systems*, Elsevier, vol. 55, pp. 312–320, 2014.

[36] X. Wang, Y. Song and M. Irving, Modern Power Systems Analysis. 2009th Edition.

APPENDIX

DATA OF THE IEEE 30-BUS SYSTEM

Table I. Bus Load of the IEEE 30-bus System

Bus	Load (MW)	Bus	Load(MW)
1	0.0	16	3.5
2	21.7	17	9.0
3	2.4	18	3.2
4	67.6	19	9.5
5	34.2	20	2.2
6	0.0	21	17.5
7	22.8	22	0.0
8	30.0	23	3.2
9	0.0	24	8.7
10	5.8	25	0.0
11	0.0	26	3.5
12	11.2	27	0.0
13	0.0	28	0.0
14	6.2	29	2.4
15	8.2	30	10.6

Table II. Line Parameters of the IEEE 30-bus System

Line	From Bus	To Bus	R (p.u)	X (p.u)	Tap Ratio	Rating (p.u)
1	1	2	0.0192	0.0575		0.300
2	1	3	0.0452	0.1852	0.9610	0.300
3	2	4	0.0570	0.1737		0.300
4	3	4	0.0132	0.0379		0.300
5	2	5	0.0472	0.1983		0.300
6	2	6	0.0581	0.1763		0.300
7	4	6	0.0119	0.0414		0.300
8	5	7	0.0460	0.1160		0.300
9	6	7	0.0267	0.0820		0.300
10	6	8	0.0120	0.0420		0.300
11	6	9	0.0000	0.2080		0.300
12	6	10	0.0000	0.5560		0.300
13	9	11	0.0000	0.2080		0.300
14	9	10	0.0000	0.1100	0.9700	0.300
15	4	12	0.0000	0.2560	0.9650	0.650
16	12	13	0.0000	0.1400	0.9635	0.650
17	12	14	0.1231	0.2559		0.320
18	12	15	0.0662	0.1304		0.320
19	12	16	0.0945	0.1987		0.320
20	14	15	0.2210	0.1997		0.160
21	16	17	0.0824	0.1932		0.160
22	15	18	0.1070	0.2185		0.160
23	18	19	0.0639	0.1293	0.9590	0.170
24	19	20	0.0340	0.0680		0.320
25	10	20	0.0936	0.2090		0.320
26	10	17	0.0324	0.0845	0.9850	0.320
27	10	21	0.0348	0.0749		0.300
28	10	22	0.0727	0.1499		0.300
29	21	22	0.0116	0.0236		0.300
30	15	23	0.1000	0.2020		0.160
31	22	24	0.1150	0.1790		0.300
32	23	24	0.1320	0.2700	0.9655	0.160
33	24	25	0.1885	0.3292		0.300
34	25	26	0.2544	0.3800		0.300
35	25	27	0.1093	0.2087		0.300
36	28	27	0.0000	0.3960		0.300
37	27	29	0.2198	0.4153	0.9810	0.300
38	27	30	0.3202	0.6027		0.300
39	29	30	0.2399	0.4533		0.300

DATA OF THE IEEE 118-BUS SYSTEM

Table I. Bus Load of the IEEE 118-bus System

Bus	Load (MW)	Bus	Load(MW)
1	54.14	60	78
2	21.23	61	0
3	41.4	62	77
4	31.85	63	0
5	0	64	0
6	55.2	65	0
7	20.17	66	39
8	0	67	28
9	0	68	0
10	0	69	0
11	74.31	70	66
12	49.89	71	0
13	36.09	72	0
14	14.86	73	0
15	95.54	74	68
16	26.54	75	47
17	11.68	76	68
18	63.69	77	61
19	47.77	78	71
20	19.11	79	39
21	14.86	80	130
22	10.62	81	0
23	7.43	82	54
24	0	83	20
25	0	84	11
26	0	85	24
27	65.82	86	21
28	18.05	87	0
29	25.48	88	48
30	0	89	0
31	45.65	90	78
32	62.63	91	0
33	24.42	92	65
34	62.63	93	12
35	35.03	94	30
36	32.91	95	42
37	0	96	38
38	0	97	15
39	27	98	34
40	20	99	0
41	37	100	37
42	37	101	22
43	18	102	5
44	16	103	23
45	53	104	38
46	28	105	31
47	34	106	43
48	20	107	28
49	87	108	2
50	17	109	8

51	17	110	39
52	18	111	0
53	23	112	25
54	113	113	0
55	63	114	8.49
56	84	115	23.35
57	12	116	0
58	12	117	21.23
59	277	118	33

Table II. Line Parameters of the IEEE 118-bus System

Line No.	From Bus	To Bus	R (pu)	X (pu)	B (pu)	Flow Limit (MW)
1	1	2	0.0303	0.0999	0.0254	175
2	1	3	0.0129	0.0424	0.01082	175
3	4	5	0.00176	0.00798	0.0021	500
4	3	5	0.0241	0.108	0.0284	175
5	5	6	0.0119	0.054	0.01426	175
6	6	7	0.00459	0.0208	0.0055	175
7	8	9	0.00244	0.0305	1.162	500
8	8	5	0	0.0267	0	500
9	9	10	0.00258	0.0322	1.23	500
10	4	11	0.0209	0.0688	0.01748	175
11	5	11	0.0203	0.0682	0.01738	175
12	11	12	0.00595	0.0196	0.00502	175
13	2	12	0.0187	0.0616	0.01572	175
14	3	12	0.0484	0.16	0.0406	175
15	7	12	0.00862	0.034	0.00874	175
16	11	13	0.02225	0.0731	0.01876	175
17	12	14	0.0215	0.0707	0.01816	175
18	13	15	0.0744	0.2444	0.06268	175
19	14	15	0.0595	0.195	0.0502	175
20	12	16	0.0212	0.0834	0.0214	175
21	15	17	0.0132	0.0437	0.0444	500
22	16	17	0.0454	0.1801	0.0466	175
23	17	18	0.0123	0.0505	0.01298	175
24	18	19	0.01119	0.0493	0.01142	175
25	19	20	0.0252	0.117	0.0298	175
26	15	19	0.012	0.0394	0.0101	175
27	20	21	0.0183	0.0849	0.0216	175
28	21	22	0.0209	0.097	0.0246	175
29	22	23	0.0342	0.159	0.0404	175
30	23	24	0.0135	0.0492	0.0498	175
31	23	25	0.0156	0.08	0.0864	500
32	26	25	0	0.0382	0	500
33	25	27	0.0318	0.163	0.1764	500
34	27	28	0.01913	0.0855	0.0216	175
35	28	29	0.0237	0.0943	0.0238	175
36	30	17	0	0.0388	0	500
37	8	30	0.00431	0.0504	0.514	175
38	26	30	0.00799	0.086	0.908	500
39	17	31	0.0474	0.1563	0.0399	175
40	29	31	0.0108	0.0331	0.0083	175
41	23	32	0.0317	0.1153	0.1173	140
42	31	32	0.0298	0.0985	0.0251	175
43	27	32	0.0229	0.0755	0.01926	175
44	15	33	0.038	0.1244	0.03194	175
45	19	34	0.0752	0.247	0.0632	175
46	35	36	0.00224	0.0102	0.00268	175
47	35	37	0.011	0.0497	0.01318	175
48	33	37	0.0415	0.142	0.0366	175
49	34	36	0.00871	0.0268	0.00568	175
50	34	37	0.00256	0.0094	0.00984	500
51	38	37	0	0.0375	0	500
52	37	39	0.0321	0.106	0.027	175
53	37	40	0.0593	0.168	0.042	175
54	30	38	0.00464	0.054	0.422	175
55	39	40	0.0184	0.0605	0.01552	175
56	40	41	0.0145	0.0487	0.01222	175
57	40	42	0.0555	0.183	0.0466	175
58	41	42	0.041	0.135	0.0344	175
59	43	44	0.0608	0.2454	0.06068	175
60	34	43	0.0413	0.1681	0.04226	175
61	44	45	0.0224	0.0901	0.0224	175
62	45	46	0.04	0.1356	0.0332	175
63	46	47	0.038	0.127	0.0316	175
64	46	48	0.0601	0.189	0.0472	175
65	47	49	0.0191	0.0625	0.01604	175

66	42	49	0.0715	0.323	0.086	175
67	42	49	0.0715	0.323	0.086	175
68	45	49	0.0684	0.186	0.0444	175
69	48	49	0.0179	0.0505	0.01258	175
70	49	50	0.0267	0.0752	0.01874	175
71	49	51	0.0486	0.137	0.0342	175
72	51	52	0.0203	0.0588	0.01396	175
73	52	53	0.0405	0.1635	0.04058	175
74	53	54	0.0263	0.122	0.031	175
75	49	54	0.073	0.289	0.0738	175
76	49	54	0.0869	0.291	0.073	175
77	54	55	0.0169	0.0707	0.0202	175
78	54	56	0.00275	0.00955	0.00732	175
79	55	56	0.00488	0.0151	0.00374	175
80	56	57	0.0343	0.0966	0.0242	175
81	50	57	0.0474	0.134	0.0332	175
82	56	58	0.0343	0.0966	0.0242	175
83	51	58	0.0255	0.0719	0.01788	175
84	54	59	0.0503	0.2293	0.0598	175
85	56	59	0.0825	0.251	0.0569	175
86	56	59	0.0803	0.239	0.0536	175
87	55	59	0.04739	0.2158	0.05646	175
88	59	60	0.0317	0.145	0.0376	175
89	59	61	0.0328	0.15	0.0388	175
90	60	61	0.00264	0.0135	0.01456	500
91	60	62	0.0123	0.0561	0.01468	175
92	61	62	0.00824	0.0376	0.0098	175
93	63	59	0	0.0386	0	500
94	63	64	0.00172	0.02	0.216	500
95	64	61	0	0.0268	0	500
96	38	65	0.00901	0.0986	1.046	500
97	64	65	0.00269	0.0302	0.38	500
98	49	66	0.018	0.0919	0.0248	500
99	49	66	0.018	0.0919	0.0248	500
100	62	66	0.0482	0.218	0.0578	175
101	62	67	0.0258	0.117	0.031	175
102	65	66	0	0.037	0	500
103	66	67	0.0224	0.1015	0.02682	175
104	65	68	0.00138	0.016	0.638	500
105	47	69	0.0844	0.2778	0.07092	175
106	49	69	0.0985	0.324	0.0828	175
107	68	69	0	0.037	0	500
108	69	70	0.03	0.127	0.122	500
109	24	70	0.00221	0.4115	0.10198	175
110	70	71	0.00882	0.0355	0.00878	175
111	24	72	0.0488	0.196	0.0488	175
112	71	72	0.0446	0.18	0.04444	175
113	71	73	0.00866	0.0454	0.01178	175
114	70	74	0.0401	0.1323	0.03368	175
115	70	75	0.0428	0.141	0.036	175
116	69	75	0.0405	0.122	0.124	500
117	74	75	0.0123	0.0406	0.01034	175
118	76	77	0.0444	0.148	0.0368	175
119	69	77	0.0309	0.101	0.1038	175
120	75	77	0.0601	0.1999	0.04978	175
121	77	78	0.00376	0.0124	0.01264	175
122	78	79	0.00546	0.0244	0.00648	175
123	77	80	0.017	0.0485	0.0472	500
124	77	80	0.0294	0.105	0.0228	500
125	79	80	0.0156	0.0704	0.0187	175
126	68	81	0.00175	0.0202	0.808	500
127	81	80	0	0.037	0	500
128	77	82	0.0298	0.0853	0.08174	200
129	82	83	0.0112	0.03665	0.03796	200
130	83	84	0.0625	0.132	0.0258	175
131	83	85	0.043	0.148	0.0348	175
132	84	85	0.0302	0.0641	0.01234	175

133	85	86	0.035	0.123	0.0276	500
134	86	87	0.02828	0.2074	0.0445	500
135	85	88	0.02	0.102	0.0276	175
136	85	89	0.0239	0.173	0.047	175
137	88	89	0.0139	0.0712	0.01934	500
138	89	90	0.0518	0.188	0.0528	500
139	89	90	0.0238	0.0997	0.106	500
140	90	91	0.0254	0.0836	0.0214	175
141	89	92	0.0099	0.0505	0.0548	500
142	89	92	0.0393	0.1581	0.0414	500
143	91	92	0.0387	0.1272	0.03268	175
144	92	93	0.0258	0.0848	0.0218	175
145	92	94	0.0481	0.158	0.0406	175
146	93	94	0.0223	0.0732	0.01876	175
147	94	95	0.0132	0.0434	0.0111	175
148	80	96	0.0356	0.182	0.0494	175
149	82	96	0.0162	0.053	0.0544	175
150	94	96	0.0269	0.0869	0.023	175
151	80	97	0.0183	0.0934	0.0254	175
152	80	98	0.0238	0.108	0.0286	175
153	80	99	0.0454	0.206	0.0546	200
154	92	100	0.0648	0.295	0.0472	175
155	94	100	0.0178	0.058	0.0604	175
156	95	96	0.0171	0.0547	0.01474	175
157	96	97	0.0173	0.0885	0.024	175
158	98	100	0.0397	0.179	0.0476	175
159	99	100	0.018	0.0813	0.0216	175
160	100	101	0.0277	0.1262	0.0328	175
161	92	102	0.0123	0.0559	0.01464	175
162	101	102	0.0246	0.112	0.0294	175
163	100	103	0.016	0.0525	0.0536	500
164	100	104	0.0451	0.204	0.0541	175
165	103	104	0.0466	0.1584	0.0407	175
166	103	105	0.0535	0.1625	0.0408	175
167	100	106	0.0605	0.229	0.062	175
168	104	105	0.00994	0.0378	0.00986	175
169	105	106	0.014	0.0547	0.01434	175
170	105	107	0.053	0.183	0.0472	175
171	105	108	0.0261	0.0703	0.01844	175
172	106	107	0.053	0.183	0.0472	175
173	108	109	0.0105	0.0288	0.0076	175
174	103	110	0.03906	0.1813	0.0461	175
175	109	110	0.0278	0.0762	0.0202	175
176	110	111	0.022	0.0755	0.02	175
177	110	112	0.0247	0.064	0.062	175
178	17	113	0.00913	0.0301	0.00768	175
179	32	113	0.0615	0.203	0.0518	500
180	32	114	0.0135	0.0612	0.01628	175
181	27	115	0.0164	0.0741	0.01972	175
182	114	115	0.0023	0.0104	0.00276	175
183	68	116	0.00034	0.00405	0.164	500
184	12	117	0.0329	0.14	0.0358	175
185	75	118	0.0145	0.0481	0.01198	175
186	76	118	0.0164	0.0544	0.01356	175